MATCHING METHODS FOR SINGLE AND MULTIPLE INTERFACES: DISCRETE AND CONTINUOUS MEDIA

F. GARCÍA-MOLINER and V.R. VELASCO

Instituto de Ciencia de Materiales, C.S.I.C., Serrano 123, 28006 Madrid, Spain

NORTH-HOLLAND

PHYSICS REPORTS (Review Section of Physics Letters) 200, No. 3 (1991) 83–125. North-Holland

MATCHING METHODS FOR SINGLE AND MULTIPLE INTERFACES: DISCRETE AND CONTINUOUS MEDIA*

F. GARCÍA-MOLINER and V.R. VELASCO

Instituto de Ciencia de Materiales, C.S.I.C., Serrano 123, 28006 Madrid, Spain

Editor: G.H.F. Diercksen Received December 1989

Contents:

Abstract:

The problem of matching arises with one or more interfaces, for example, from a free surface or simple heterojunction to a superlattice. A method to solve these problems is discussed with emphasis on the practical aspects. The formalism, based on Green functions, is general at first and then branches off as one considers continuous media – requiring differential calculus – or discrete media – requiring finite differences. Appropriate concepts of transfer matrices are introduced with which the practical problems of evaluating the intervening Green functions can be speedily solved. Practical algorithms for evaluating the different transfer matrices are presented.

* Originally commissioned for Computer Physics Reports.

Single orders for this issue

PHYSICS REPORTS (Review Section of Physics Letters) 200, No. 3 (1991) 83–125.

Copies of this issue may be obtained at the price given below. All orders should be sent directly to the Publisher. Orders must be accompanied by check.

Single issue price Dfl. 33.00, postage included.

0 370-1573/91/$15.05

1. Introduction: the SGFM method

Surface physics constitutes a very active field of research in both the applied and basic aspects. The same holds for interfaces, the free surface being a particular case. Many problems of interest involve more than one interface, for example, a layer on a substrate, a sandwich type of system, including the very important case of quantum wells, a multiple quantum well or a superlattice. This field has grown into a vast area of very active developments, experimental as well as theoretical, on account of the many practical applications of such composite laminar systems.

One may be interested in different types of states or elementary excitations, for example, electronic states, phonons, magnons, piezoelectric waves and many others, but in all these cases there are some basic common features. From a theoretical point of view the one-interface system poses the problem of *matching*, whether one matches electronic wavefunctions or, say, vibration amplitudes. The essential feature of composite laminar systems is that the various interfaces are coupled and this raises the problem of interrelated multiple matching. Now, for the present purpose the constituent materials can be classified in *continuous* and *discrete* media, depending on the type of mathematics employed in their description. We shall consider these separately.

Continuous media are studied with differential calculus. For planar geometry we introduce the following notation: the position vector is $\boldsymbol{r} = (\boldsymbol{\rho}, z)$, where $\boldsymbol{\rho} = (x, y)$ is the two-dimensional (2D) position vector in the plane of the interfaces and z is the coordinate in the perpendicular direction. The wavevector is $\boldsymbol{k} = (\boldsymbol{\kappa}, k_z)$, where $\boldsymbol{\kappa} = (k_x, k_y)$. The initial differential equations are Fourier transformed in the 2D surface plane and we are left with $\boldsymbol{\kappa}$-dependent 2D ordinary differential equations in the variable z. Henceforth, the $\boldsymbol{\kappa}$-dependence will be understood everywhere if not explicitly indicated. The problem may involve one or several coupled differential equations, depending on the number N of components of the field under study. Examples of $N = 1$ are the electrostatic potential – Poisson equation – or the electronic wavefunction – Schrödinger equation for a one-band model. For $N = 2$ we have, for instance, a two-band envelope function model for electronic states, electromagnetic matching or elastic waves in a sagittal geometry. $N = 3$ could be the problem of elastic waves with arbitrary geometry and $N = 4$, for instance, the case of piezoelectric modes in which the electrostatic potential and the three vibration amplitudes are coupled. An envelope function four-band model would be another example of $N = 4$ and more elaborate ones are used in practice, up to $N = 14$. Perhaps the most important case can be typified by an arbitrary pseudopotential model. In the corresponding plane-wave representation the Schrödinger equation then becomes a system of N coupled differential equations. From a mathematical point of view the general problem under study is that of matching a field of N components subject to N coupled ordinary differential equations, that is we study $N \times N$ linear differential matrices acting on the N-component vectors to be matched.

Discrete media are described in terms of ordinary matrix algebra. For instance, phonons in a discrete lattice or electronic states in a tight-binding model. In this case the position variable is discrete, corresponding to atomic positions and, after the 2D Fourier transform, to the 1D atomic layer position in the direction perpendicular to the interfaces. The three vibration amplitudes or the atomic states forming the basis of the tight-binding scheme are also labelled by discrete indices and in the end we have $N \times N$ matrices acting on N-component vectors. But now no differential calculus is involved and so matching must be effected differently.

Many techniques have been and are being developed for doing matching calculations for single or multiple interfaces, for continuous or discrete systems and for different types of elementary excitations. There has been too much progress in this area to even attempt to review it here. This paper is only

concerned with the presentation of one such technique, the surface Green function matching (SGFM) method, with which the different cases can be treated with a unified point of view. The emphasis will be on the formulae to be used and on the algorithms which, combined with these, provide a technique for doing practical calculations.

The problem will be formulated in terms of Green functions. Let $\boldsymbol{G}_M$, in general a matrix, be "the Green function (GF) of each constituent medium M". This requires further specification, as will be seen presently. Let $\boldsymbol{G}_s$ be the Green function of the composite matched system under study. The problem is to obtain $\boldsymbol{G}_s$ in terms of the constituent $\boldsymbol{G}_M$, assumed to be all known. All $\boldsymbol{G}$ are functions of κ, of an eigenvalue Ω – which can be energy E, or ω^2, for instance – and of a continuous or discrete position variable. We shall see how $\boldsymbol{G}_s$ can be obtained in terms of the constituent $\boldsymbol{G}_M$ but, having done this, the real question is how the $\boldsymbol{G}_M$ are evaluated.

Consider an ideal interface (fig. 1). Two unperturbed bulk crystals are ideally cleaved and matched without perturbation. Then each $\boldsymbol{G}_M$ is the unperturbed GF of the corresponding bulk crystal. If the model is fairly realistic, that is complicated, the evaluation of each $\boldsymbol{G}_M$ may require quite substantial computation. For instance, the direct evaluation of the spectral representation of a GF involves the evaluation of rather complicated integrals with oscillatory factors in the integrand. This question will be addressed later.

In some cases the difficulties are of a different nature. Consider the situations described in fig. 2. The bulk models are now extremely simple, but the presence of inhomogeneities on both sides of the matching plane raises a new question. What are $\boldsymbol{G}_1$ and $\boldsymbol{G}_2$ now? How are they defined and evaluated? When this is combined with the complications of elaborate bulk-crystal models the problem may easily become quite formidable. These issues will also be discussed here.

The paper is organised as follows. Sections 2 through 6 cover the case of continuous media, when differential calculus is involved, and sections 7 through 10 are devoted to discrete media. In both cases

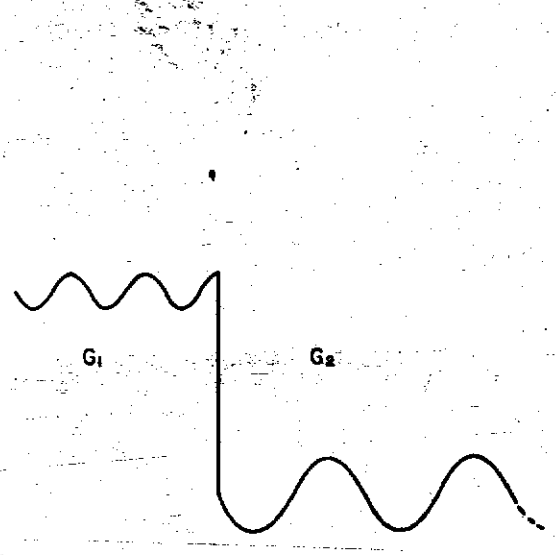

Fig. 1. Model of an ideal interface. G_1 and G_2 are the corresponding bulk-crystal Green functions.

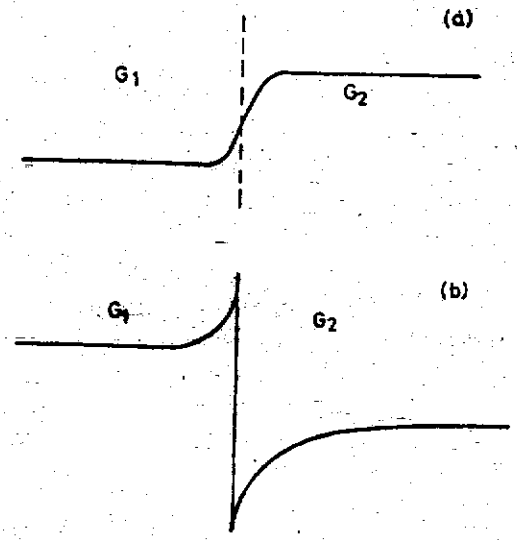

Fig. 2. Qualitative pictures of (a) self-consistent potential barrier at a free surface or an interface (jellium model) and (b) a semiconductor heterojunction with inversion layers (one-band effective-mass model). The first question now concerns the definition of G_1 and G_2.

the discussion starts with the formulation of the matching problem in terms of the SGFM analysis. Since the formalism has been presented elsewhere, only a summary is given here, with emphasis on the formulae to be used. For continuous media this is done in section 2 for a single interface and in section 3 for multiple interfaces, while for discrete media, single interfaces are discussed in section 7 and multiple interfaces in section 8. The question of the evaluation of the intervening GF is then discussed, in section 4 for continuous media and in section 9 for discrete media. Except for some occasional appeal to a specific case, the discussion up to this point is general and applicable to any type of elementary excitation. Some examples are given to illustrate practical applications to continuous and discrete media, together with discussions of practical aspects. Final comments are made in section 10.

A brief collection of background material on the SGFM method may be useful. This method was initially developed for electronic surface or interface states [1–4] and then extended to film-like problems involving two interfaces [5–9]. Planar geometry is nearly always involved, but this is not necessary [9, 10]. The method has also been extended to the study of electronic states at twin faults in metals [11] and of tunnelling problems [12]. The relationship to the phase shift analysis is discussed in refs. [2, 9, 13–15]. As stressed above, the method is not restricted to the case of one-electron states. Surface plasmons, for instance, were discussed early on in terms of SGFM [16, 17] and so were some many-body aspects of surface or interface problems in Hartree [18], Thomas–Fermi [19] and random-phase [20] approximations. Discussions of this method in general terms can be found in refs. [9, 14, 21]. The relationship to the concept of surface electromagnetic impedance has been discussed in refs. [9, 22] and there have also been further developments extending the scope to other physical problems, such as elastic surface or interface waves [6, 23, 24], surface thermodynamics [23, 25], viscoelastic waves involving fluid surfaces or interfaces [26–28], piezoelectric surface or interface waves [29, 30] and magnetoelastic surface waves [31, 32]. The SGFM analysis has been lately extended to the case of quantum wells and superlattices [33] and used to study elastic [34] and piezoelectric [35] waves in superlattices, as well as the electro-optical properties of quantum wells [36]. Another extension has been recently made to the study of elementary excitations in superconducting systems involving interfaces [37].

All the above references concern continuous systems. For discrete media the SGFM analysis was initially formulated and used for surface phonons [38–41]. A general formulation, valid for any discrete system, can be found in refs. [42, 43]. This has been used to study the electronic structure of semiconductor interfaces [44, 45] and transition-metal surfaces [46], as well as the surface magnetism in transition metals [47]. The general formalism for layered systems of the type of quantum wells and superlattices can be found in refs. [43, 48]. Applications have been made to study phonons in graphite intercalation compounds [49] and in metallic superlattices [50], and also to the study of the electronic structure of semiconductors [51] and metallic superlattices [52]. These applications also contain further additions to the formal development of the SGFM analysis and to the formulae used for its practical implementation.

2. Continuous media: single interface

We consider the matching surface at $z = 0$, with medium 1 on the left-hand side and medium 2 on the right-hand side. As explained in the introduction we assume $\boldsymbol{G}_1$ and $\boldsymbol{G}_2$ to be known. The question of their evaluation will be addressed later. We collect here the main formulae of the SGFM analysis following the notation established in the introduction. Details of their derivation can be found in the

above references. All the objects appearing here and henceforth can be matrices but this will be understood without explicit matrix notation except when it becomes convenient.

Let $\mathcal{G}$ denote the surface projection ($z = z' = 0$) of any Green function $\boldsymbol{G}$, be it $\boldsymbol{G}_1$, $\boldsymbol{G}_2$ or $\boldsymbol{G}_s$. We define its inverse *in the 2D space of the projection surface*, that is

$$\mathcal{G}\mathcal{G}^{-1} = \mathcal{G}^{-1}\mathcal{G} = \mathcal{I}\,, \tag{2.1}$$

where $\mathcal{I}$ is the unit of the 2D space of the surface. Let $'\boldsymbol{G}$ denote $\partial \boldsymbol{G}(z, z')/\partial z$. For second-order differential equations the first derivative has a discontinuity. We define

$$'\mathcal{G}^{(\pm)} = \lim_{z' \to \pm 0} \left[\frac{\partial G(z, z')}{\partial z} \right]_{z=0}. \tag{2.2}$$

The discontinuity

$$\Delta' \mathcal{G} = '\mathcal{G}^{(+)} - '\mathcal{G}^{(-)} = S \tag{2.3}$$

is obtained by performing a first integration of the differential equation defining the GF under study. We recall that this term may denote a differential matrix, in which case $\boldsymbol{G}$, $\mathcal{G}$, $'\mathcal{G}^{\pm}$ and $\boldsymbol{S}$ are matrices. The point is that $\boldsymbol{S}$ *is known*. This fact will be used later.

2.1. The matched Green function G_s

Now, let z_1 (z_2) denote the variable z when it is on side 1 (2), and likewise for z'. Then

$$G_s(z_1, z_2') = G_1(z_1, 0)\mathcal{G}_1^{-1}\mathcal{G}_s\mathcal{G}_2^{-1}G_2(0, z_2')\,; \tag{2.4}$$

$$G_s(z_2, z_2') = G_2(z_2, z_2') + G_2(z_2, 0)\mathcal{G}_2^{-1}(\mathcal{G}_s - \mathcal{G}_2)\mathcal{G}_2^{-1}G_2(0, z_2')\,. \tag{2.5}$$

We also recall that the dependence on $(\boldsymbol{\kappa}, \Omega)$ is understood throughout. For incidence from side 2 the reflection and transmission amplitudes are, respectively,

$$f_R = (\mathcal{G}_s - \mathcal{G}_2)\mathcal{G}_2^{-1}\,, \qquad f_T = \mathcal{G}_s\mathcal{G}_2^{-1}\,. \tag{2.6}$$

A dual set of formulae holds with 1 and 2 interchanged.

The secular equation for matching states is

$$\det|\mathcal{G}_s^{-1}(\boldsymbol{\kappa}, \Omega| = 0\,. \tag{2.7}$$

This yields the surface or interface dispersion relations $\Omega(\boldsymbol{\kappa})$, that is an electronic surface band structure, for instance.

Spectral functions of various types constitute an important class of objects of physical interest. With the present sign convention the general density of states formula for the matched system reads

$$N(\Omega) = -\frac{1}{\pi}\,\mathrm{Im}\,\mathrm{Tr}\,G(\Omega^+)\,, \quad \Omega^+ = \lim_{\varepsilon \to 0}(\Omega + \mathrm{i}\varepsilon)\,. \tag{2.8}$$

Consistently with this there are different spectral functions of interest, which correspond to different definitions. Firstly, there are κ-dependent spectral functions, for example, the local density of states (LDOS)

$$N_\kappa(\Omega, z) = -\frac{1}{\pi} \operatorname{Im} \operatorname{Tr} G_s(\kappa, \Omega^+; z, z) . \tag{2.9}$$

In particular, the LDOS at the interface is

$$\mathcal{N}_\kappa(\Omega) = -\frac{1}{\pi} \operatorname{Im} \operatorname{Tr} \mathcal{G}_s(\kappa, \Omega^+) . \tag{2.10}$$

For a free surface this would be the key spectral function to study the inelastic cross section for scattering of an incoming probe off the surface as in, for example, surface Brillouin scattering [53] or inelastic ultrasonic scattering [54], while for the local charge density the quantity required is the integrated LDOS

$$N(\Omega, z) = \int \frac{d^2\kappa}{(2\pi)^2} N_\kappa(\Omega, z) . \tag{2.11}$$

For the total density of states we must integrate (2.11) over z. The result can be cast in the form

$$\begin{aligned} N(\Omega) = & -\frac{1}{\pi} \operatorname{Im} \operatorname{Tr} \int_{-\infty}^{0} dz\, G_1(\Omega^+; z, z) - \frac{1}{\pi} \operatorname{Im} \operatorname{Tr} \int_{0}^{\infty} dz\, G_2(\Omega^+; z, z) \\ & + \frac{1}{\pi} \operatorname{Im} \operatorname{Tr} \int_{-\infty}^{0} dz\, G_1(\Omega^+; z, 0) \mathcal{G}_1^{-1}(\Omega^+) G_1(\Omega^+; 0, z) \\ & + \frac{1}{\pi} \operatorname{Im} \operatorname{Tr} \int_{0}^{\infty} dz\, G_2(\Omega^+; z, 0) \mathcal{G}_2^{-1}(\Omega^+) G_2(\Omega^+; 0, z) - \frac{1}{\pi} \frac{d \arg \det |\mathcal{G}_s^{-1}(\Omega^+)|}{d\Omega} . \end{aligned} \tag{2.12}$$

As with the other spectral functions, this can be read either for a fixed κ or else integrated over κ as in (2.11).

The task then is to find $\mathcal{G}_s$, on which all these formulae rest.

2.2. *The matching formula*

In order to obtain $\mathcal{G}_s$ we must specify the matching conditions. This requires going into the physics of each particular case. For instance, for a one-band effective-mass model of electronic states the matching conditions are continuity of the wavefunction ψ and of $m^{-1}\psi'$. Furthermore, the discontinuity S of (2.3) is $-2m/\hbar^2$. The matching formula is then

$$\mathcal{G}_s^{-1} = \mathcal{S}_1^{-1} \cdot \mathcal{G}_1^{(+)} \mathcal{G}_1^{-1} - \mathcal{S}_2^{-1} \cdot \mathcal{G}_2^{(-)} \mathcal{G}_2^{-1} . \tag{2.13}$$

This can be cast in a general form that encompasses the different particular cases. From the derivatives

$'\mathscr{G}^{(\pm)}$ we define appropriate linear differential forms $\mathscr{A}^{(\pm)}$, which correspond to the physical magnitudes one must match, for example, for the scalar Schrödinger equation $\mathscr{A}^{(\pm)}$ is $m^{-1}{}'\mathscr{G}^{(\pm)}$. Then the discontinuity (2.3) can be cast in the form

$$\Delta\mathscr{A} = \mathscr{A}^{(+)} - \mathscr{A}^{(-)} = C\,, \tag{2.14}$$

where C ($= -2/\hbar^2$ in this example) is a constant independent of the medium. Then the matching formula reads

$$\mathscr{G}_s^{-1} = C^{-1}(\mathscr{A}_1^{(+)}\mathscr{G}_1^{-1} - \mathscr{A}_2^{(-)}\mathscr{G}_2^{-1})\,. \tag{2.15}$$

In this form this holds for any physical system. We need only specify C and the form of $\mathscr{A}$ in each case. Here are some examples of physical interest.

(i) *Electrostatics*. G represents the electrostatic potential. $C = -4\pi$ in Gaussian units. $\mathscr{A}^{(\pm)} = \varepsilon'\mathscr{G}^{(\pm)}$ represents the normal component of the electric displacement vector.

For problems involving more than one component we use (x_1, x_2, x_3) instead of (x, y, z) and $\nabla_i = \partial/\partial x_i$, so ∇_3 is the normal derivative.

(ii) *A two-component problem: electromagnetic waves*. G represents the electric field E, $C = -4\pi/c$ (Gaussian units) and $\mathscr{A}^{(\pm)}$ is a 2×2 matrix defined after

$$A_{ij} = \frac{c}{i\omega}(\nabla_i G_{3j} - \nabla_3 G_{ij})\,, \quad i, j = 1, 2 = x, y\,. \tag{2.16}$$

These represent the tangential components of the magnetic induction B. Note that $\nabla_3 G_{ij}$ is the normal derivative $'G_{ij}$, which, upon projection, yields the discontinuous derivatives $'\mathscr{G}^{(\pm)}$, whence $\mathscr{A}^{(\pm)}$. All matrices involved in (2.15) are in this case 2×2.

(iii) *A three-component problem: elastic waves*. G represents vibration amplitudes. $C = -1$ and

$$A_{ij} = c_{3ikn}\nabla_k G_{nj}\,, \quad i, j, k, n = 1, 2, 3\,. \tag{2.17}$$

Summation over repeated indices is implied, the c_{3ikn} are the elastic stiffness coefficients with the first index equal to 3, corresponding to the normal coordinate z and when $k = 3$, then $\nabla_k G_{nj} = {}'G_{nj}$, whence $'\mathscr{G}_{nj}^{(\pm)}$ and finally $\mathscr{A}^{(\pm)}$. This represents stresses.

(iii) *A four-component problem: piezoelectric waves*. Here G is a 4×4 matrix representing the elastic and electrostatic fields coupled through the piezoelectric coefficients e_{ijk}. We use Latin indices to span the values 1, 2, 3, corresponding to the three vibration amplitudes, and Greek indices $\alpha, \beta = 1, 2, 3, 4$. The value 4 corresponds to the electrostatic potential, the fourth component of the field under study. Then

$$A_{i\beta} = c_{3ikn}\nabla_k G_{n\beta} + e_{k3i}\nabla_k G_{4\beta}\,, \qquad A_{4\beta} = e_{3kn}\nabla_k G_{n\beta} - \varepsilon_{3k}\nabla_k G_{4\beta}\,. \tag{2.18}$$

In this case $C = -1$, that is

$$(\Delta\mathscr{A})_{\alpha\beta} = \mathscr{A}_{\alpha\beta}^{(+)} - \mathscr{A}_{\alpha\beta}^{(-)} = -\delta_{\alpha\beta}\,, \quad \alpha, \beta = 1, 2, 3, 4\,. \tag{2.19}$$

All matrices entering the matching formula (2.15) are then 4×4.

It will be observed that $\mathscr{A}^{(\pm)}\mathscr{G}^{-1}$ is always a surface impedance and the theorem (2.7) embodies the principle of matching of surface impedances with the convention that the normal to the surface has the same sign – from negative to positive – for the two media.

Arbitrary values of N may appear in electronic structure calculations based on either envelope function models or else more elaborate ones, such as pseudopotentials. These require separate consideration. The use of envelope function models for matching problems raises several questions concerning their validity and scope and, especially, the matching conditions. Different views have been put forward [55] and further arguments continue to appear in the literature [56]. The purpose here is not to discuss models but ways to solve a given matching problem. So our standpoint is that a certain Hamiltonian has been adopted and our task is to solve the corresponding matching problem. Ultimately the N-component vector $\boldsymbol{f}$ under study is subject to a given matrix differential equation. Although higher-order derivatives may be used in other models we shall consider here second-order differential equations for which a prototype eigenvalue equation can be

$$\boldsymbol{H}\cdot\boldsymbol{f}=\left[-\frac{\mathrm{d}}{\mathrm{d}z}\boldsymbol{K}\frac{\mathrm{d}}{\mathrm{d}z}+\frac{1}{2}\left(\boldsymbol{D}\frac{\mathrm{d}}{\mathrm{d}z}+\frac{\mathrm{d}}{\mathrm{d}z}\boldsymbol{D}\right)+\boldsymbol{L}\right]\cdot\boldsymbol{f}=\Omega\boldsymbol{f}\,, \tag{2.20}$$

with $\boldsymbol{K}$, $\boldsymbol{D}$ and $\boldsymbol{L}$ possibly being z-dependent. Then

$$\mathscr{A}^{(\pm)}=\mathscr{K}\cdot{}'\mathscr{G}^{(\pm)}-\mathscr{D}\cdot\mathscr{G}\,,\qquad \boldsymbol{C}=\boldsymbol{I}\,. \tag{2.21}$$

A pseudopotential model can be regarded as a representative example of an advanced type of model, capable of embodying a good description of the electronic band structure. Although this is not the only type of accurate model one can devise, and several others have been put forward for matching calculations [57], the general line of argument is sufficiently illustrated by the study of a Hamiltonian of the form

$$H=-\frac{\hbar^2}{2m}\nabla^2+V(\boldsymbol{r})\,,\quad V(\boldsymbol{r})=\sum_{\boldsymbol{g}}V_{\boldsymbol{g}}\exp(\mathrm{i}\boldsymbol{g}\cdot\boldsymbol{r})\,. \tag{2.22}$$

Write down separately the $\boldsymbol{\rho}$-dependence and the z-dependence, for example,

$$\begin{aligned}V(\boldsymbol{r})&=\sum_{\boldsymbol{\gamma}}V_{\boldsymbol{\gamma}}(z)\exp(\mathrm{i}\boldsymbol{\gamma}\cdot\boldsymbol{\rho})\,,\\ \psi_{\boldsymbol{k}}(\boldsymbol{r})&=\sum_{\boldsymbol{\gamma}}\psi_{\boldsymbol{\kappa}+\boldsymbol{\gamma}}(z)\exp[\mathrm{i}(\boldsymbol{\kappa}+\boldsymbol{\gamma})\cdot\boldsymbol{\rho}]\,,\end{aligned} \tag{2.23}$$

where the $\boldsymbol{\gamma}$ are the 2D projections of the 3D reciprocal lattice vectors $\boldsymbol{g}$. Take the corresponding 2D plane-wave representation and leave the z-dependence in the differential form. Then the system of differential equations is

$$\sum_{\boldsymbol{\gamma}'}\left[\left(E-\frac{\hbar^2}{2m}|\boldsymbol{K}+\boldsymbol{\gamma}|^2+\frac{\hbar^2}{2m}\frac{\mathrm{d}^2}{\mathrm{d}z^2}\right)\delta_{\boldsymbol{\gamma},\boldsymbol{\gamma}'}-V_{\boldsymbol{\gamma}-\boldsymbol{\gamma}'}(z)\right]\psi_{\boldsymbol{\kappa}+\boldsymbol{\gamma}'}(z)=0\,, \tag{2.24}$$

$$\mathscr{A}^{\pm} = m^{-1}\mathscr{g}^{(\pm)}, \qquad C = -\frac{2}{\hbar^2} I, \tag{2.25}$$

where I is the $N \times N$ unit matrix, N being the number of resulting coupled differential equations.

The above suffices to demonstrate the wide range of problems that can be treated in a unified way. In each case one must find $\mathscr{A}^{\pm}$ and C. The matching formula is then (2.15) which, used in (2.4), (2.5) through (2.12) allows us to evaluate practically all objects of interest concerning one single surface or interface.

3. Continuous media: multiple interfaces

We now consider problems involving more than one interface. As prototypes we shall consider two cases. One is that of two interfaces. Examples of physical interest can be a sandwich-type structure consisting of three media 1–2–3 with their respective matching interfaces. Then medium 2 has a finite thickness. If 1 and 3 are equal, then this corresponds to a quantum well. If one of the extreme media is the vacuum – say, 1 – then it corresponds to a layer of a material, 2, on top of a substrate of another material. The other case we shall consider is the superlattice ...1–2–1–2..., in which the two constituent media alternate in a periodic way. We then have an alternating sequence of 1–2 and 2–1 interfaces. Other laminar systems, such as polytype superlattices, can be treated by an extension of the same method.

3.1. *The sandwich or quantum well case*

Consider the configuration shown in fig. 3a: three media with two interfaces labelled l (left) and r (right). Each P_M is the projector onto the corresponding domain. The symbols l and r will be used

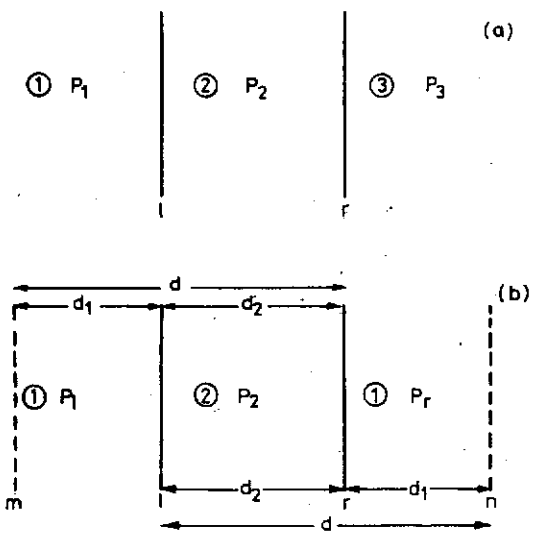

Fig. 3. Notation for (a) a sandwich or quantum well and (b) a superlattice.

indiscriminately either as labels or else to indicate the units of the corresponding 2D surface spaces. For instance, a projection at l will be described by

$$\mathcal{G}_l\,, \quad \mathcal{G}_l^{-1}\mathcal{G}_l = \mathcal{G}_l\mathcal{G}_l^{-1} = l\,. \tag{3.1}$$

Likewise, G_{lr} denotes the matrix element of G between l and r. We recall that the quantities appearing in the formulae to be collected here can in general be matrices, for example, G, $\mathcal{G}_l$, G_{lr}, but explicit matrix notation will not be used unless it is necessary or convenient for clarity. However, the correct order of all factors will always be maintained. Now, given G_2 and G_s we define the complete interface or projection domain with projector $\mathcal{I} = l + r$ and the 2×2 supermatrix projections

$$\tilde{G}_2 = \begin{pmatrix} \mathcal{G}_{2l} & G_{2lr} \\ G_{2rl} & \mathcal{G}_{2r} \end{pmatrix}, \qquad \tilde{G}_s = \begin{pmatrix} \mathcal{G}_{sl} & G_{slr} \\ G_{srl} & \mathcal{G}_{sr} \end{pmatrix}, \tag{3.2}$$

together with their inverses:

$$\tilde{G}_2^{-1}\tilde{G}_2 = \tilde{G}_2\tilde{G}_2^{-1} = \begin{pmatrix} l & 0 \\ 0 & r \end{pmatrix} = \tilde{G}_s^{-1}\tilde{G}_s = \tilde{G}_s\tilde{G}_s^{-1}\,. \tag{3.3}$$

We furthermore define the external and internal projectors

$$P_e = P_1 + P_3\,, \qquad P_i = P_2 \tag{3.4}$$

and the external Green function

$$P_eG_eP_e = \begin{pmatrix} P_1G_1P_1 & 0 \\ 0 & P_3G_3P_3 \end{pmatrix}. \tag{3.5}$$

This is a compact way of expressing the fact that in G_1 both z and z' are in domain 1, while in G_3 they are in domain 3. The complete interface projection of G_e is

$$\tilde{G}_e = \begin{pmatrix} \mathcal{G}_{1l} & 0 \\ 0 & \mathcal{G}_{3r} \end{pmatrix}. \tag{3.6}$$

It is more useful to write down the SGFM formulae for the two-interface problem with the more compact projector notation. The results are then isomorphic with those of the one-interface case, the one side and the other side being in correspondence with the *in*side and the *out*side. For instance, for z outside (P_e) and z' inside (P_i), the formula is

$$P_eG_sP_i' = P_eG_e\tilde{G}_e^{-1}\tilde{G}_s\tilde{G}_2^{-1}G_2P_2'\,, \tag{3.7}$$

which is isomorphic with (2.4) if we put $P_1G_sP_2$ instead of $G_s(z_1, z_2')$ and likewise for the rest. But here z can be in either P_1 or P_3 and both cases are encompassed by the compact formula (3.7). Symbols with tildes are projections – defined in (3.2) through (3.6) – and can be understood as containing $\mathcal{I}$ as a prefactor and as a postfactor. Thus a term like $P_eG_e\tilde{G}_e^{-1}$ can be read as $P_eG_e\mathcal{I}\tilde{G}_e^{-1}$. The meaning of $P_eG_e\mathcal{I}$ is the following: suppose z is in P_1. Then this is the two-component row vector

$$P_e G_e \mathcal{I} = [G_1(z, l), 0], \tag{3.8}$$

while for z in P_3:

$$P_e G_e \mathcal{I} = [0, G_3(z, r)]. \tag{3.9}$$

Here $G(z, l/r)$ means that z' is at l/r. For the same reason the factor $G_2 P_2'$ can be read as $\mathcal{I} G_2 P_2'$ and this is the column vector

$$\mathcal{I} G_2 P_2' = \begin{pmatrix} G_2(l, z_2') \\ G_2(r, z_2') \end{pmatrix}, \tag{3.10}$$

whereas $P_2 G_e \mathcal{I}$ is the row vector

$$P_2 G_2 \mathcal{I} = [G_2(z, l), G_2(z, r)] \tag{3.11}$$

and this appears in the formula

$$P_2 G_s P_2 = P_2 G_2 P_2 + P_2 G_2 \tilde{G}_2^{-1} (\tilde{G}_s - \tilde{G}_2) \tilde{G}_2^{-1} G_2 P_2, \tag{3.12}$$

which is isomorphic with (2.5). As in the one-interface case, a dual set of formulae holds with internal and external interchanged.

The next question is the matching formula for $\tilde{G}_s^{-1}$, and this is

$$\tilde{G}_s^{-1} = C^{-1} (\tilde{\mathcal{A}}_e \tilde{G}_e^{-1} - \tilde{\mathcal{A}}_2 \tilde{G}_2^{-1}), \tag{3.13}$$

where $\tilde{\mathcal{A}}_e$ and $\tilde{\mathcal{A}}_2$ are 2×2 supermatrices corresponding to $\tilde{\mathcal{A}}_1^{(+)}$ and $\tilde{\mathcal{A}}_2^{(-)}$ of the one-interface case. The general relationship between $\tilde{\mathcal{A}}^{(\pm)}$ and ${}'\tilde{\mathcal{G}}^{(\pm)}$ has been discussed in section 2.2, thus it suffices to discuss the supermatrices formed simply from the Green function derivatives. These are

$${}'\tilde{G}_e = \begin{pmatrix} {}'\mathcal{G}_{1l}^{(+)} & 0 \\ 0 & -{}'\mathcal{G}_{3r}^{(-)} \end{pmatrix}, \qquad {}'\tilde{G}_2 = \begin{pmatrix} {}'\mathcal{G}_{2l}^{(-)} & {}'\mathcal{G}_{2l}^{(+)} \mathcal{G}_{2l}^{-1} G_{2lr} \\ -{}'\mathcal{G}_{2r}^{(-)} \mathcal{G}_{2r}^{-1} G_{2rl} & -{}'\mathcal{G}_{2r}^{(+)} \end{pmatrix}. \tag{3.14}$$

By combining the Green function derivatives with appropriate coefficients corresponding to each particular case we go from ${}'\tilde{G}_e$ and ${}'\tilde{G}_2$ to $\tilde{\mathcal{A}}_e$ and $\tilde{\mathcal{A}}_2$.

Now, the internal Green function can be chosen to satisfy arbitrary boundary conditions at the l- and r-interfaces provided neither corresponds to an infinite barrier [58]. Thus, with this sole restriction, one can choose from a double infinity of Green functions G_2, all satisfying the same differential equations in P_2 and arbitrary boundary conditions at l and r. In particular, if we can find a G_2 satisfying

$${}'\mathcal{G}_{2l}^{(+)} = {}'\mathcal{G}_{2r}^{(-)} = 0, \tag{3.15}$$

then ${}'\tilde{G}_2$ becomes diagonal, and so does $\tilde{\mathcal{A}}_2$, whence a substantial simplification in the algebra may ensue.

3.2. The superlattice

The notation is laid out in fig. 3b. Here m and n denote another two interfaces and d is the length of the period. This entails a phase factor $f = \exp(iqd)$ for states with (super)momentum q associated with the superperiodicity of period d. The internal projector, and corresponding Green function continue to be P_2 and $P_2G_2P_2$, but the external domain now has projector

$$\hat{P} = P_l + P_r\,, \tag{3.16}$$

with P_l and P_r also spanning finite domains. The material contained in these is the same, but they carry left and right labels. The extension of the objects defined in section 3.1 is as follows: define, for z in P_l or P_r,

$$\begin{aligned} &P_lG_el = G_1(z_l, l)\,, \qquad P_lG_er = f^{-1}P_lG_1m = f^{-1}G_1(z_l, m)\,, \\ &P_rG_el = fP_rG_1n = fG_1(z_r, n)\,, \qquad P_rG_er = G_r(z_r, r)\,, \end{aligned} \tag{3.17}$$

whence the 2×2 supermatrix

$$\hat{P}G_eI = \begin{pmatrix} P_lG_el & P_lG_er \\ P_rG_el & P_rG_er \end{pmatrix} = \begin{pmatrix} G_l(z_l, l) & f^{-1}G_1(z_l, m) \\ fG_1(z_r, n) & G_1(z_r, r) \end{pmatrix}. \tag{3.18}$$

The complete interface projection is then

$$\hat{G}_e = \begin{pmatrix} \mathscr{G}_{el} & G_{elr} \\ G_{erl} & \mathscr{G}_{er} \end{pmatrix} = \begin{pmatrix} \mathscr{G}_{1l} & f^{-1}G_1(l, m) \\ fG_1(r, n) & \mathscr{G}_{1r} \end{pmatrix}. \tag{3.19}$$

Note the appearance of non-diagonal terms, with corresponding phase factors, in the supermatrices corresponding to external objects.

The SGFM formulae are now typified by

$$\hat{P}G_sP_i' = \hat{P}G_e\hat{G}_e^{-1}\tilde{G}_s\tilde{G}_2^{-1}G_2P_2\,, \tag{3.20}$$

$$P_iG_sP_i = P_2G_2P_2 + P_2G_2\tilde{G}_2^{-1}(\tilde{G}_s - \tilde{G}_2)\tilde{G}_2^{-1}G_2P_2\,, \tag{3.21}$$

which are again isomorphic with the corresponding formulae for the one- and two-interface problems. An alternative formula for $\hat{P}G_s\hat{P}$ is discussed in ref. [51].

The next question is again the matching formula for $\tilde{G}_s$, which involves the corresponding derivatives. As in section 3.1 we need only discuss the 2×2 supermatrices involving derivatives of the Green functions. Obviously $'\tilde{G}_2$ is the same as in (3.14), but now instead of $'\tilde{G}_e$ we have

$$'\hat{G}_e = \begin{pmatrix} '\mathscr{G}_{1l}^{(+)} & f^{-1}\,'\mathscr{G}_{1l}^{(-)}\mathscr{G}_{1l}^{-1}G_1(l, n) \\ -f\,'\mathscr{G}_{1r}^{(+)}\mathscr{G}_{1r}^{-1}G_1(r, n) & -'\mathscr{G}_{1r}^{(-)} \end{pmatrix}. \tag{3.22}$$

From this we form the corresponding $\hat{\mathscr{A}}_e$ and hence obtain the matching formula for the superlattice

$$\tilde{G}_s^{-1} = C^{-1}(\hat{\mathcal{A}}_e \hat{G}_e^{-1} - \tilde{\mathcal{A}}_2 \tilde{G}_2^{-1}) . \tag{3.23}$$

As before, G_1 in each domain can be chosen arbitrarily provided it satisfies the same differential equations inside P_l or P_r. In particular, the choice

$${}'\mathcal{G}_{1l}^{(-)} = {}'\mathcal{G}_{1r}^{(+)} = 0 \tag{3.24}$$

makes ${}'\hat{G}_e$ diagonal, thus simplifying the algebra.

4. Evaluation of Green functions and SGFM formulae for continuous media

The practical use of the formulae so far presented, and of others one can obtain from a SGFM analysis of various matching problems raises the question of the evaluation of the intervening G. Ignoring for the moment some of the problems commented on in connection with fig. 1, the practical issue is the evaluation of G for a given medium.

If G can be obtained in analytical form as $G(\boldsymbol{k})$, that is $G(\boldsymbol{\kappa}, k_z)$, then all terms entering the above formulae are readily evaluated from

$$G(\boldsymbol{\kappa}, z - z') = \int_{-\infty}^{\infty} \frac{dk_z}{2\pi} G(\boldsymbol{\kappa}, k_z) \exp[ik_z(z - z')] \tag{4.1}$$

and from

$${}'\mathcal{G}^{(\pm)} = \lim_{\eta \to 0} \int_{-\infty}^{\infty} \frac{dk_z}{2\pi} G(\boldsymbol{\kappa}, k_z) \exp(\mp ik_z \eta) . \tag{4.2}$$

This assumes an ideal junction of the two unperturbed bulk media which remain homogeneous right up to the matching surface. This is typically a good physical model for problems involving long waves, for example, elastic, piezoelectric or magnetoelastic waves. Even if one includes specific surface effects, for example, surface stresses, in the long-wave limit these are essentially localised perturbations going like $\delta(z)$ and there is no difficulty in including them in the analysis [6, 9, 26, 27, 28, 59, 60]. A similar case is that of a thin layer on a substrate provided the thickness h of the layer is such that $\kappa h \ll 1$ for the long waves – small κ – of interest [61]. By Fourier transforming the equations of motion one can find $G(\boldsymbol{k})$ and then, by using (4.1) and (4.2), one can implement the SGFM analysis in practice.

Figure 4 shows some results obtained in this way in the study of surface Brillouin scattering for GaAs (110) surfaces [60]. One can obtain not only the form of the cross section but also the parts contributed by the spectral strength corresponding to vibrations perpendicular and parallel to the surface. Figure 5 shows the phase velocity of the surface waves on Si (001) surfaces compared with data obtained from inelastic ultrasonic diffraction experiments. The phase velocities are plotted as a function of the angle formed by the propagation vector $\boldsymbol{\kappa}$ with the [100] axis, both contained in the (001) surface. In this case one can also follow the evolution of the surface mode while describing it with a great deal of spectral information. Details can be found in ref. [24].

As an example of a superlattice system, fig. 6 shows some calculated dispersion relations for elastic

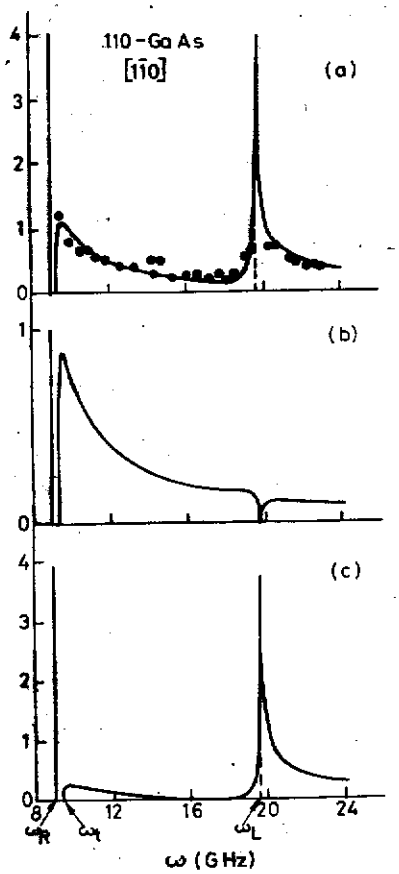

Fig. 4. (a) Theoretical spectrum for Brillouin scattering in the [1$\bar{1}$0] direction of the (110) surface of GaAs. Dots denote experimental measurements. (b) Transverse contribution to the theoretical spectrum. (c) Longitudinal contribution to the theoretical spectrum.

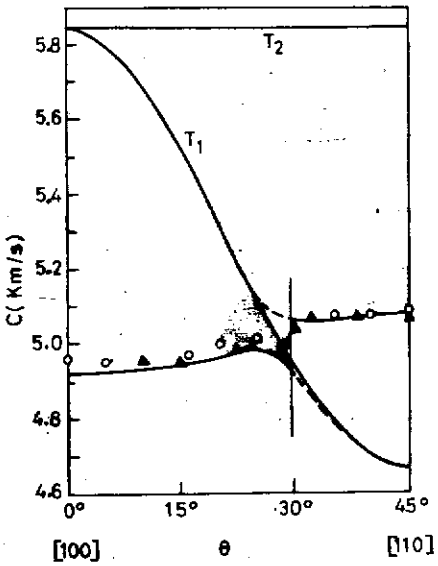

Fig. 5. Surface-wave velocities as a function of direction on the (001) Si surface. Open circles and full triangles represent ultrasonic scattering data. The vertical line indicates the approximate direction where one of the branches should cease while the other should start to predominate.

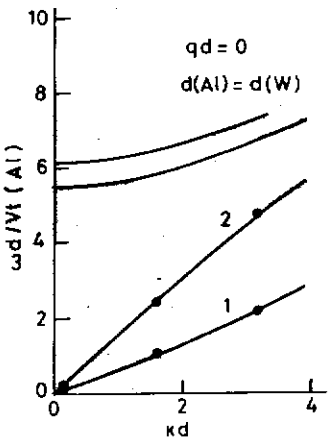

Fig. 6. Dispersion relations for sagittal waves in the W–Al (001) superlattice with $q = 0$, $\kappa \| [100]$ and $d(\mathrm{Al}) = d(\mathrm{W})$.

waves in a W–Al superlattice [34]. Two aspects of these waves can be of interest. One is that, in general, waves propagating parallel to interfaces are in principle sagittal, that is, part of the vibration amplitude is longitudinal and part is transverse, perpendicular to both the interface and the corresponding wavevector, just as in fig. 4. The interest then lies in knowing how the total spectral strength is distributed between the two polarisations. The other aspect of interest is the spatial distribution of the spectral strength given by (2.9). For an electronic wavefunction this would be proportional to $|\psi|^2$. Figure 7 shows the corresponding spectral functions for three different frequencies spanning the two lowest branches of fig. 6. One can see, for instance, that the first branch is nearly all transverse and the second one nearly all longitudinal, as in bulk material, but the modes have different preferential confinements in real space. Again, one can study at will different modes and configurations and obtain detailed spectral information [24].

A viscoelastic fluid can be formally treated in a way that is mathematically isomorphic with that of an isotropic elastic solid medium [9, 26–28]. A quantity of interest is the fractional change $\Delta V/V_0$ of the surface wave velocity V_0 of a free solid surface, which changes to a different value V when the solid is "loaded" with a fluid. Table 1 shows experimental and calculated results obtained from an SGFM calculation [26].

The situation is rather more involved when it comes to problems involving electronic states. The bulk Green function is of course trivially easy for free-electron states and this offers already some interesting

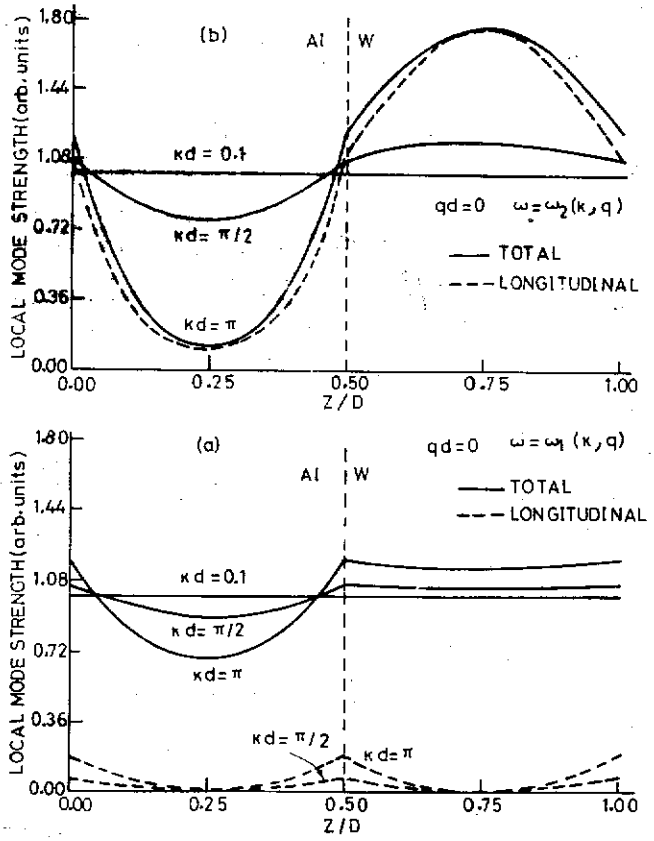

Fig. 7. Spatial dependence of the mode strength (local density of states) for the three modes $\omega(\kappa d, qd)$ of the two branches: (a) ω_1, (b) ω_2, of fig. 6. Arbitrary units. The left-hand side $0 < z/d < 0.5$, is the Al layer. The longitudinal strength for $\omega_1(0.1, 0)$ is negligible, as is the difference between the total and longitudinal strengths for $\omega_2(0.1, 0)$ and $\omega_2(\pi/2, 0)$.

Table 1
Fractional changes in surface wave velocities because of fluid loading

	Theory (%)	Experiment (%)
Al/water	0.46	0.50
Al/glycerine	1.65	1.10
Steel/water	0.05	0.06
Steel/glycerine	0.18	0.13

possibilities, such as the study of some collective aspects of a metallic electron gas bounded by a surface [17–20]. Crystallinity complicates the evaluation of G, but this can be done with simple pseudopotentials without great effort. In a plane-wave representation, when a given wavevector $\boldsymbol{k}$ mixes with several reciprocal lattice vectors g, G becomes a matrix labelled by g, g'. In the 2D projection for the surface problem one ends up with matrices labelled by γ, γ', as in (2.24). For metals one can study in this way, for instance, the electronic structure of solid solutions of simple metals [62] or localised states at twin faults and surfaces [11]. For semiconductors one can also evaluate the bulk G and use these to study surface states, but so far this has been done mainly for simple pseudopotential models and ideally terminated surfaces [63]. While these calculations were useful in the early stages in the theory of surface states, the issues of today require more accurate calculations. If the bulk model is more accurate, hence more complicated, the evaluation of the G and their derivatives requires very substantial numerical effort, and more so if one wants to do a self-consistent calculation [64].

Moreover, there may be situations in which it is not even clear how the bulk G is to be defined. A point in case is, for instance, that of a parabolic quantum well [65]. We now address these problems.

4.1. *The transfer matrix M*

Transfer matrices for solutions of systems of ordinary differential equations can be defined in different ways and various definitions can be found in the literature. Basically one can define a matrix that transfers either amplitudes or both amplitudes and derivatives. The former can be useful if the (vector) wavefunction can be expressed as a combination of a set of known functions. Then if suffices to know the amplitudes. We shall soon see that the latter is more convenient for the practical implementation of the SGFM method under quite general conditions. We shall follow the analysis of ref. [66] with only a rearrangement of terms which we shall presently explain.

Consider a system of N coupled differential equations. The differential operator and the Green function are $N \times N$ matrices. The wavefunction is an N-component vector f. Let f_p $(p = 1, 2, \ldots, N)$ be these components. Physically they could correspond, say, to vibration amplitudes, to the envelope functions of a many-band model or to the Fourier components in a plane-wave representation for a pseudopotential model. The formal analysis holds quite generally. We define the $2N$-component vector $\boldsymbol{F}$, associated with f, by

$$\boldsymbol{F}(z) = \begin{pmatrix} F_1(z) \\ F_2(z) \\ \vdots \\ F_N(z) \\ F_{N+1}(z) \\ \vdots \\ F_{2N}(z) \end{pmatrix} = \begin{pmatrix} f_1(z) \\ f_2(z) \\ \vdots \\ f_N(z) \\ f_1'(z) \\ \vdots \\ f_N'(z) \end{pmatrix} \tag{4.3}$$

We then define the $2N \times 2N$ transfer matrix $\boldsymbol{M}$ which transfers F from z_0 to z:

$$\boldsymbol{F}(z) = \boldsymbol{M}(z, z_0) \cdot \boldsymbol{F}(z_0) . \tag{4.4}$$

We shall use $p, q = 1, 2, \ldots, N$ to denote components of $\boldsymbol{G}$ or $\boldsymbol{f}$ and $i, j = 1, 2, \ldots, 2N$ to denote components of $\boldsymbol{M}$ or $\boldsymbol{F}$. In the definition used in ref. [66] amplitudes f_p and derivatives f'_p occupied an alternating sequence $(f_1, f'_1, f_2, f'_2, \ldots)$ but here we shall use the order defined in (4.3). This order is optional and simplifies the notation.

The first question is to relate $\boldsymbol{G}$ and $\boldsymbol{M}$. A preliminary formulation for $N = 1$ (G a scalar, $\boldsymbol{M}$ a 2×2 matrix) was presented in ref. [58] and a full analysis of this case in ref. [67]. The extension to $N = 2$ can be found in ref. [37] and the general analysis for arbitrary N in ref. [68]. We now summarise the results.

Consider the $2N \times 2N$ matrix $\boldsymbol{M}$ of elements M_{ij}. We then define four $N \times N$ submatrices resulting from the partitioning of $\boldsymbol{M}$ in blocks:

$$\left(\begin{array}{ccc|ccc} M_{1,1} & \cdots & M_{1,N} & M_{1,N+1} & \cdots & N_{1,2N} \\ \vdots & & \vdots & \vdots & & \vdots \\ M_{N,1} & \cdots & M_{N,N} & M_{N,N+1} & \cdots & M_{N,2N} \\ \hline M_{N+1,1} & \cdots & M_{N+1,N} & M_{N+1,N+1} & \cdots & M_{N+1,2N} \\ \vdots & & \vdots & \vdots & & \vdots \\ M_{2N,1} & \cdots & M_{2N,N} & M_{2N,N+1} & \cdots & M_{2N,2N} \end{array}\right) = \left(\begin{array}{c|c} \boldsymbol{M}_{AA} & \boldsymbol{M}_{AD} \\ \hline \boldsymbol{M}_{DA} & \boldsymbol{M}_{DD} \end{array}\right) . \tag{4.5}$$

Then $\boldsymbol{M}_{AA}$ relates the amplitude at z to the amplitude at z_0, $\boldsymbol{M}_{AD}$ relates amplitudes at z to derivatives at z_0, and so on. The elements and derivatives of the constituent Green functions can be fully obtained in terms of the submatrices of (4.5). The details have been given elsewhere, ref. [68]. Here we give a summary of the results.

Taking a given reference point $z = 0$ where matching is eventually to be effected and defining

$$\boldsymbol{M}_{\alpha\beta}(\pm) = \boldsymbol{M}_{\alpha\beta}(\pm\infty, 0) , \tag{4.6}$$

the transfer matrices sweep through the potentials or similar coefficients of the corresponding domains. These constitute the input to the evaluation of the corresponding $\boldsymbol{M}$, which depend on the eigenvalue variable Ω. For propagating states this is to be understood in the sense of the causal limit Ω^+. Consider now the matching formula (2.13). The quantities of interest are the logarithmic derivatives. We denote

$$\boldsymbol{\mathcal{L}}_1^{(+)} = {}'\boldsymbol{\mathcal{G}}_1^{(+)} \cdot \boldsymbol{\mathcal{G}}_1^{-1} = \boldsymbol{T}_1^{-1} , \qquad \boldsymbol{\mathcal{L}}_2^{(-)} = {}'\boldsymbol{\mathcal{G}}_2^{(-)} \cdot \boldsymbol{\mathcal{G}}_2^{-1} = \boldsymbol{V}_2^{-1} , \tag{4.7}$$

then

$$\boldsymbol{T}_1^{-1} = -[\boldsymbol{M}_{AD}(-)^{-1} \cdot \boldsymbol{M}_{AA}(-)]_1 , \qquad \boldsymbol{V}_2^{-1} = -[\boldsymbol{M}_{AD}(+)^{-1} \cdot \boldsymbol{M}_{AA}(+)]_2 . \tag{4.8}$$

The label 1 or 2 indicates the domain swept by the corresponding transfer matrices. The secular matrix (2.13) is thus fully obtained in terms of constituent transfer matrices only. It is now convenient to introduce the following notation: let $\boldsymbol{M}$ denote a matrix that can be a complex function of a complex variable:

$$\boldsymbol{M}(\Omega) = \boldsymbol{a}(\Omega) + \mathrm{i}\boldsymbol{b}(\Omega)\,. \tag{4.9}$$

Define $\bar{\boldsymbol{M}}$, $\bar{\boldsymbol{a}}$ and $\bar{\boldsymbol{b}}$ as the transposes of $\boldsymbol{M}$, $\boldsymbol{a}$ and $\boldsymbol{b}$. Then we define

$$\bar{\boldsymbol{M}}_{\mathrm{c}}(\Omega) = \bar{\boldsymbol{a}}(\Omega) - \mathrm{i}\bar{\boldsymbol{b}}(\Omega)\,. \tag{4.10}$$

Note that Ω is not conjugated, so for complex Ω this is not quite the Hermitian conjugate of $\boldsymbol{M}$. Now, of the complete matched $\boldsymbol{G}_{\mathrm{s}}(z, z')$ the two configurations of interest in practice are (i) z and z' on opposite sides, for example, to study transmission across the interface – and (ii) z and z' on the same side and usually $z = z'$ – for example, to study a local density of states. For instance, for $z \le 0 \le z'$:

$$\boldsymbol{G}_{\mathrm{s}}(z, z') = [\boldsymbol{M}_{\mathrm{AA}}(z,0) + \boldsymbol{M}_{\mathrm{AD}}(z,0)\cdot\boldsymbol{T}_1^{-1}]\cdot\mathscr{G}_{\mathrm{s}}\cdot[\boldsymbol{M}_{\mathrm{AA}}(z',0) + \boldsymbol{V}_2^{-1}\cdot\boldsymbol{M}_{\mathrm{AD}}(z',0)]\,, \tag{4.11}$$

while for z and z' equal and on the same side:

$$\begin{aligned}
\boldsymbol{G}_{\mathrm{s}}(z,z) &= [\boldsymbol{M}_{\mathrm{AA}}(z,0) + \boldsymbol{M}_{\mathrm{AD}}(z,0)\cdot\boldsymbol{T}_1^{-1}]\cdot\{\mathscr{G}_{\mathrm{s}}\cdot[\bar{\boldsymbol{M}}_{\mathrm{cAA}}(z,0) + \boldsymbol{U}_1^{-1}\cdot\bar{\boldsymbol{M}}_{\mathrm{cAD}}(z,0)] - \boldsymbol{S}_1\cdot\bar{\boldsymbol{M}}_{\mathrm{cAD}}(z,0)\}\,,\\
\boldsymbol{G}_{\mathrm{s}}(z,z) &= [\boldsymbol{M}_{\mathrm{AA}}(z,0) + \boldsymbol{M}_{\mathrm{AD}}(z,0)\cdot\boldsymbol{V}_2^{-1}]\cdot\{\mathscr{G}_{\mathrm{s}}\cdot[\bar{\boldsymbol{M}}_{\mathrm{cAA}}(z,0) + \boldsymbol{Q}_2^{-1}\cdot\bar{\boldsymbol{M}}_{\mathrm{cAD}}(z,0)]\\
&\qquad - \boldsymbol{S}_2\cdot\bar{\boldsymbol{M}}_{\mathrm{cAA}}(z,0)\}\,,
\end{aligned} \tag{4.12}$$

where

$$\boldsymbol{U}_1^{-1} = -[\bar{\boldsymbol{M}}_{\mathrm{cAA}}(-)\cdot\bar{\boldsymbol{M}}_{\mathrm{cAD}}(-)^{-1}]_1\,, \qquad \boldsymbol{Q}_2^{-1} = -[\bar{\boldsymbol{M}}_{\mathrm{cAA}}(+)\cdot\boldsymbol{M}_{\mathrm{cAD}}(+)^{-1}]_2\,. \tag{4.13}$$

The label 1 or 2 indicates the domain for which the transfer matrices are evaluated.

The same considerations hold for multiple matching. For instance, for the 1–2–3 system discussed in section 3.1 one finds

$$\tilde{\boldsymbol{G}}_{\mathrm{s}}^{-1} = \begin{pmatrix} \boldsymbol{S}_1^{-1}\cdot\boldsymbol{T}_1^{-1} & 0 \\ 0 & -\boldsymbol{S}_3^{-1}\cdot\boldsymbol{V}_3^{-1} \end{pmatrix} + \tilde{\boldsymbol{G}}_2^{-1}\,, \tag{4.14}$$

where $\boldsymbol{T}_1$ is given by (4.8) with the reference point at l and $\boldsymbol{V}_2$ is also given by (4.8) with 2 replaced by 3 and the reference point at r. Furthermore,

$$\tilde{\boldsymbol{G}}_2^{-1} = \begin{pmatrix} \boldsymbol{m}_{\mathrm{DA}}^{-1}\cdot\mathbf{m}_{\mathrm{DD}}\cdot\boldsymbol{S}_2 & \boldsymbol{m}_{r\mathrm{DA}}^{-1}\cdot\boldsymbol{S}_2 \\ \boldsymbol{m}_{\mathrm{DA}}^{-1}\cdot\boldsymbol{S}_2 & \boldsymbol{m}_{\mathrm{AA}}\cdot\boldsymbol{m}_{\mathrm{DA}}\cdot\boldsymbol{S}_2 \end{pmatrix}, \tag{4.15}$$

where

$$m_{r\alpha\beta} = M_{\alpha\beta}(l, r)\,, \tag{4.16}$$

which transfer *from* r to l. This is a submatrix of the inverse of $M(l, r)$ but it can also be directly evaluated by feeding the same potentials in the reverse order, starting from r. A similar formula holds for the superlattice, only the first matrix of (4.14) has then non-diagonal terms containing the phase factor $\exp(\mathrm{i}qd)$, where q is the 1D wavevector associated with the periodicity d of the superlattice. The

complete $\boldsymbol{G}_s(z, z')$ can also be obtained, for either the sandwich structure or the superlattice, by using the appropriate SGFM formulae and relating the intervening Green functions to the corresponding $\boldsymbol{M}$ [68]. The point is that in all cases everything is ultimately expressed in terms of transfer matrices, which can be evaluated directly from the differential system by means of efficient numerical algorithms.

Consider, for instance, a parabolic quantum well. Medium 1 is taken to be a homogeneous material right up to l. Medium 3 is equal to medium 1 from r onwards. Medium 2 has a parabolic potential profile from l to r. This is then the difficult region. Suppose one uses a one-band effective-mass model. Then G_1 and G_3 are obtained trivially and hence $\mathscr{L}^{(\pm)}$ for each case. But G_2 is much harder. In fact it would be hopeless to try and evaluate it in order to use (3.14) in (3.13). This could be even worse for any other arbitrary potential profile. However, formula (4.15) solves this problem. It suffices to evaluate the transfer matrix, for which efficient numerical algorithms exist and the problem of evaluating or even defining G_2 has been circumvented altogether. Table 2 shows some results obtained for a parabolic quantum well of $Al_xGa_{1-x}As$ with graded composition, that is with x varying from l to r. The eigenvalues were calculated by using (4.14) and (4.15). In this case the $m_{\alpha\beta}$ are scalars ($m_{AA} = m_{11}$, $m_{AD} = m_{12}$, $m_{DA} = m_{21}$, $m_{DD} = m_{22}$). The calculation was done [58] with a personal computer and the results compared with those of an elaborate full computer calculation [65].

An example with $N = 2$ is the study of elementary excitations in superconductors. In Bogolioubov's model, widely used in the literature – for example, [69–71] – this involves two coupled differential equations for the electron and hole wavefunctions. If Δ is the energy gap of the superconductor, then no elementary excitation can exist with energy $E < \Delta$. However, it was found [69] that a N/S bilayer (N, normal; S, superconductor) can have elementary excitations at energies below Δ. This proximity effect was also studied in refs. [70, 71] with the same conclusion. In all these studies the spectral function evaluated was the density of states of the entire N/S bilayer. A Bardeen–Cooper–Schrieffer (BCS)-like peak appears at some low energy $E_0 < \Delta$, that is, the normal metal becomes, by the proximity effect, something like a superconductor with a very small gap equal to E_0. For a bilayer in which each layer has a thickness 30ξ, where ξ is the coherence length of the superconductor, this peak appears [37, 70] at about $E_0 = 0.09\Delta$ – the normal metal is like an almost zero-gap superconductor. This can be disclosed in real space by calculating the local spectral strength (2.9). Figure 8 shows the results of such a calculation in which the SGFM formulae were evaluated in terms of the corresponding transfer matrices [37] for $\kappa = 0$. The idea is to probe the system at an energy of interest. Figure 8a shows the local spectral strength for $E = 1.08\Delta$, slightly above the threshold at which the BCS peak appears. This demonstrates the typical spatial behaviour of this type of elementary excitation. In fig. 8b the system was probed at $E = 0.09\Delta$, where the BCS-like peak appears. The behaviour corresponds to that of an elementary excitation of the same kind and quickly decays on getting into the superconduct-

Table 2
Quantised sub-band levels for the parabolic quantum well of $Al_xGa_{1-x}As$ described in the text

Quantised sub-band level	Energy (meV) of level					
	lowest conduction		heavy holes		light holes	
	Pötz and Ferry [65]	this work	Pötz and Ferry [65]	this work	Pötz and Ferry [65]	this work
E_1	1531.1	1531.1	−4.5	−4.5	−10.1	−10.1
E_2	1555.0	1554.8	−13.4	−13.4	−30.4	−30.4
E_3	1578.8	1578.6	−22.3	−22.4	−49.6	−50.6
E_4	1601.9	1602.3	−31.2	−31.3	−68.9	−70.8

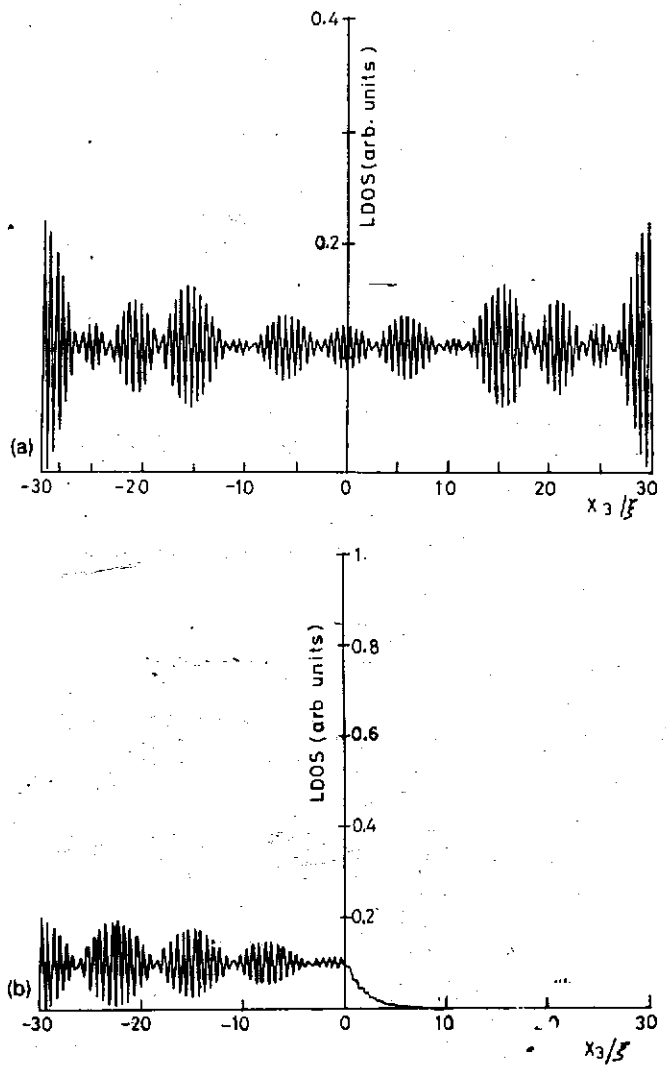

Fig. 8. (a) Spatial dependence of the spectral strength for $\kappa = 0$, $E \approx 1.08\Delta_2$, for a uniform superconductor layer of total thickness 60ξ. (b) Both layers have a thickness of 30ξ. On the left $\Delta_1 = 0$ (normal metal). Spatial dependence of the spectral strength for $\kappa = 0$, $E = 0.08\Delta_2$. Compare with (a).

ing slab, as it must since in the superconductor the energy is far below the gap threshold. The decay in fact is very steep, corresponding to E/Δ very small. The curious result is that the spectral strength of such an excitation tends to pile up not near the interface, but rather towards the far end, thirty coherence lengths away from the interface. This is another example of the kind of detailed information these calculations can yield. In this case the transfer matrix is 4×4 and can be written down analytically in terms of trigonometric functions and the calculation can also be done on a personal computer.

The use of transfer matrices to evaluate Green functions opens an interesting practical possibility to perform self-consistent calculations. If one starts from an ideal interface – two unperturbed media joined at the matching surface – whether one uses the intervening G directly or (4.6) depends on the model. If this is sufficiently tractable, then the direct evaluation of the G may be the most

Table 3
The four lowest eigenvalues for the Si inversion layer. The prime indicates the beginning of a different ladder [72]. Energy values in eV

	E_0	E_1	E_2	E_0'
Present calculation	0.058	0.091	0.110	0.088
Stern [72]	0.059	0.093	0.112	0.090

straightforward way. However, this is clearly not the case in the situations described in fig. 2. In such cases the use of M is very practical. The calculation proceeds in exactly the same way irrespective of the details of the numerical input – that is the potential profile. Thus the new potential obtained at successive stages of a self-consistent calculation can be treated in the same way and, from this point of view, the problem is straightforward except for the possible complications of the self-consistent analysis itself. As an example we can consider the inversion layer at the Si–SiO_2 interface. In this case it suffices to use a Hartree approximation [72]. Table 3 shows the results of ref. [72] and those obtained with the method discussed here [37]. The point is that the latter can be obtained with a personal computer.

5. The wavefunction of a matched system

For some physical problems one may want to know the wavefunction explicitly. This may be required to evaluate some appropriate matrix element for, say, optical transitions or electron–phonon scattering probabilities.

The SGFM analysis constitutes an extension of ordinary scattering theory in the sense that all scattering events are classified in reflection and transmission. The relationships involving Green functions are of the Dyson type. Correspondingly, there are relationships of the Lippman–Schwinger type involving the wavefunctions.

Consider the case of one single interface. Let $\phi_1(z)$ be the wavefunction of an eigenstate of medium 1 incident from the left. The corresponding ***scattering state*** wavefunction of the matched system is

$$\psi_s(z) = \phi_1(z) + G_1(z,0)\mathcal{G}_1^{-1}(\mathcal{G}_s - \mathcal{G}_1)\mathcal{G}_1^{-1}\phi_1(0), \quad z \le 0\,,$$

$$\psi_s(z) = G_2(z,0)\mathcal{G}_2^{-1}\psi_s(0) = G_2(z,0)\mathcal{G}_1^{-1}\mathcal{G}_s\mathcal{G}_1^{-1}\phi_1(0) \quad z \ge 0\,, \tag{5.1}$$

with similar formulae with 1 and 2 interchanged when the state is incident from the right.

For a bound state:

$$\psi_s(z) = G_1(z,0)\mathcal{G}_1^{-1}\psi_s(0) \quad z \le 0\,,$$

$$\psi_s(z) = G_2(z,0)\mathcal{G}_2^{-1}\psi_s(0) \quad z \ge 0\,. \tag{5.2}$$

Having related the Green functions to the transfer matrices, one can now evaluate the desired wavefunctions from the M.

The case of multiple interfaces, notably the quantum well and the superlattice, can also be ultimately referred to one single amplitude at one chosen matching surface by using various relationships obtained from the SGFM analysis [36, 68]. Note that while the z-dependence of the wavefunction is given on

by terms of the form $G(z, 0)$, the other factors are also important, as they contain, for instance, an extra dependence on the eigenvalue and possibly other important parameters. A case in point is the electro-optical properties of a quantum well in an external electric field $\mathscr{E}$. Then one is interested in the $\mathscr{E}$-dependence of ψ_s and this is contained not only in the Green function terms but also in the amplitude factor. In such cases this must be found by normalisation.

Figure 9 gives the results of a calculation [36] performed in this way, compared with experimental data on quenching of the photoluminescence of a quantum well as a function of $\mathscr{E}$. Except for the highest fields the main factor is the increasingly separate confinements of the electron and hole wavefunctions as $\mathscr{E}$ increases. The quantity calculated in this case is the overlap integral

$$\langle \psi(\text{electron}) | \psi(\text{hole}) \rangle ,$$

for which the complete $\mathscr{E}$-dependence must be obtained, and this includes the amplitude factor which can be obtained by normalising each wavefunction. For any non-trivial case this must be done numerically but is otherwise straightforward for bound states. Scattering states are different. They are normalised in the sense of δ-functions – of the energy – and this cannot be done numerically in a direct manner. In this case one can obtain the normalisation amplitudes by equating the density of states obtained from the ψ to the same quantity obtained from G. A case in point is that of a superlattice, for which all states are simultaneously matching and scattering states. Taking, say, the l surface as $z = 0$, the general formula is then

$$\psi_s(z) = G_s(z) \mathscr{G}_s^{-1} \psi_s(0) . \tag{5.3}$$

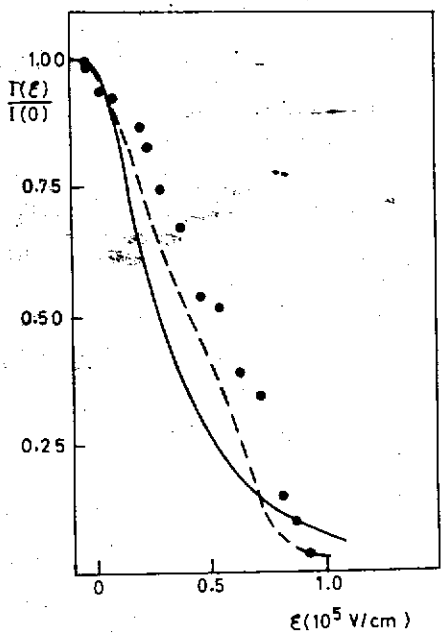

Fig. 9. The integrated photoluminescence intensity against electric field, normalised with respect to zero-field conditions. Full circles, experimental results; continuous line, variational calculation of the overlap between electron and hole wavefunctions; broken curve: SGFM calculation

6. Continuous media: practical aspects

The usefulness of the method just described rests on using a good numerical algorithm to obtain the transfer matrix. Basically we are interested in the solution of a set of N coupled linear second-order differential equations. Let this be of the general form

$$\boldsymbol{A}\cdot f'' + \boldsymbol{B}\cdot f' + (\boldsymbol{C} - EI_N) = 0\,, \quad f = \begin{pmatrix} f_1(z) \\ f_2(z) \\ \vdots \\ f_N(z) \end{pmatrix}. \tag{6.1}$$

We assume that $\boldsymbol{A}$ causes no special problem, which is usually the case in practice. This is easily transformed into a system of $2N$ coupled first-order differential equations:

$$\boldsymbol{F}' = \boldsymbol{P}\cdot\boldsymbol{F}\,, \quad \boldsymbol{P} = \begin{pmatrix} 0 & I_N \\ \boldsymbol{A}^{-1}\cdot(EI_N - \boldsymbol{C}) & -\boldsymbol{A}^{-1}\cdot\boldsymbol{B} \end{pmatrix}, \quad F = \begin{pmatrix} f_1(z) \\ f_2(z) \\ \vdots \\ f_N(z) \\ f_1'(z) \\ \vdots \\ f_N'(z) \end{pmatrix}. \tag{6.2}$$

We have defined the $2N$-component vector F. Then $\boldsymbol{P}$ is a $2N \times 2N$ matrix. The transfer matrix, defined by (4.4) is then in fact the matrix that transfers the solution of the system (6.2).

If the coefficients are constant then $\boldsymbol{M}$ can be obtained from refs. [66, 73]

$$\boldsymbol{M}(z, z_0) = \exp[\boldsymbol{P}\times(z - z_0)] \tag{6.3}$$

Obviously the matrix $\boldsymbol{P}$ can be diagonalised by means of the standard subroutines existing in mathematical subroutine libraries like EISPACK [74] and LINPACK [75]. In any case it is well known that to obtain the exponential of an arbitrary matrix is a tricky problem [76]. It is also well known that in the case of non-Hermitian matrices standard diagonalisation procedures can run into serious trouble. When the coefficients are not constant it is always possible to introduce a grid of closely spaced points such that in each narrow interval of the grid the coefficients are taken as constants. The transfer matrix for each interval is obtained according to (6.4) and then

$$\boldsymbol{M}(z, z_0) = \boldsymbol{M}(z, z - \Delta)\cdots\boldsymbol{M}(z + 2\Delta, z + \Delta)\cdot\boldsymbol{M}(z + \Delta, z_0)\,. \tag{6.4}$$

This involves repeated multiplication on top of diagonalisation and exponentiation of matrices and the amount of memory required grows very quickly with N. Moreover, this is not a very accurate procedure.

All these problems can be avoided if the transfer matrix is obtained by numerically integrating from z_0 to z the system of differential equations (6.2) and assuming at the starting point canonical basis solutions, for example,

(6.5)

where i represents a particular component and j represents a particular vector in the basis. The integration of a first-order differential system like (6.2) can be efficiently performed by using the Adams–Rashforth–Moulton method [77, 78]. From the formal point of view we need only the values of $F_j(z_0)$ to know the solution in the whole domain of interest. When starting from a canonical basis (6.5) each one of the $2N$ solutions thus obtained gives, at the variable point z, a column of the transfer matrix.

This works efficiently and for realistic cases in which N is of medium size ($N \sim 20$) it performs accurately and quickly on personal computers of the AT or XT classes.

7. Discrete media: single interface

The general introduction to the formal SGFM analysis is as in the continuous case. The *form* of the results is also the same, except that formulae like (2.4, 2.5) are to be read in terms of discrete layer indices, rather than continuous variables (z or z'). A convenient notation in terms of projectors will soon be introduced. The dependence on the eigenvalue and on the two-dimensional wavevector $\boldsymbol{\kappa}$ is again understood everywhere. All objects appearing here and henceforth can be matrices. This will also be understood without using explicit matrix notation, unless it proves convenient to do so. Details can be found in ref. [42].

For discrete media it proves convenient to use the concept of *the principal layer*. This is defined so that: (i) one principal layer interacts only with itself and with its two nearest-neighbour principal layers and this accounts for all the interactions in the crystal, (ii) the crystal is reproduced by translations of the principal layer. One principal layer may contain one or more atomic layers, depending on the geometry and on the range of interactions included in the model. After the Fourier transform parallel to the interfaces one *atomic* layer is described with as many basis states as are needed to describe the states of one atom. This determines the size of the diagonal term, a matrix in general, representing the local layer projection of, say, a Hamiltonian or a Green function matrix. If the principal layer contains two atomic layers, then the size of the matrix representing the principal-layer projection is doubled, and so on. In the following the term *layer* will be simply used to denote a principal layer.

The formal analysis to be presented here holds for any system with inherently discrete structure in which the basis states are labelled with discrete indices $(\boldsymbol{R}, \mu)$, $\boldsymbol{R}$ being a discrete atomic position. For electrons in tight binding (TB) μ labels the atomic or atomic-like states on a given atom; for phonons $\mu = x, y, z$, labels the three independent vibration amplitudes; for, say, a Heisenberg Hamiltonian, $\mu = \pm$ labels spin states, etc. Let I be the complete unit or projector of all the states in which all the atoms forming the system under study are described. For example, I could be the unit of a complete crystal. In this space one can define, in a concise notation applicable to different discrete systems, the "Hamiltonian" H and its resolvent or Green function G,

$$(\Omega - H)G = I \,. \tag{7.1}$$

This must be specified in each particular application. For electrons $\Omega = E$, for phonons $\Omega = \omega^2$, etc. Also, in the case of phonons one must keep in mind that the symbol H in an explicit calculation stands for the matrix of force constants $\phi_{\mu\nu}(\boldsymbol{R}, \boldsymbol{R}')$.

It will be necessary to include some additional notation appropriate for the discrete character of the situations to be discussed later. The situation is sketched in fig. 10. Let H_s denote the Hamiltonian of

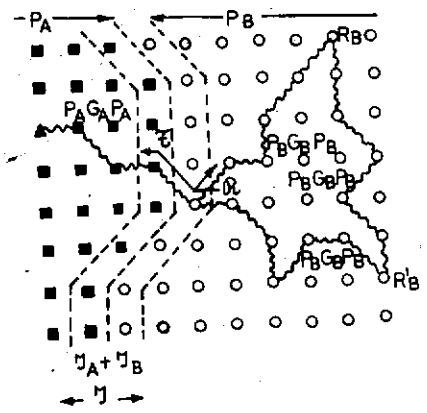

Fig. 10. An interface with A atoms (■) on one side and B atoms (○) on the other. The interface domain $\mathcal{I}$ consists of the two subdomains $\mathcal{I}_A$, part of P_A, and $\mathcal{I}_B$, a part of P_B.

the system with an interface, defined in the space of the actual existing atoms forming the system under study, and G_s its resolvent defined in the same space

$$(\Omega - H_s)G_s = P\,, \tag{7.2}$$

where P is the projector of the space of the existing atoms and in our case is spanned by

$$P = P_A + P_B\,. \tag{7.3}$$

Within P there is an *interface domain* with projector $\mathcal{I}$ consisting of two parts $\mathcal{I}_A + \mathcal{I}_B$. A *surface object* $\mathcal{N}$ is defined to exist and have an inverse, if not singular, within the space of $\mathcal{I}$

$$\mathcal{N} \equiv \mathcal{I}N\mathcal{I}\,, \qquad \mathcal{N}^{-1} \equiv \mathcal{I}N^{-1}\mathcal{I}\,, \qquad \mathcal{N}\mathcal{N}^{-1} = \mathcal{N}^{-1}\mathcal{N} = \mathcal{I}\,. \tag{7.4}$$

Now, every bulk Hamiltonian H_M ($M = A, B$) or resolvent G_M is only meaningful in the I_M part of I, that is when evaluated at the atoms M. Thus only the $\mathcal{I}_M G_M \mathcal{I}_M$ part of $\mathcal{I}G_M\mathcal{I}$ is non-vanishing. For example, viewed in the entire domain, by definition

$$\mathcal{G}_A = \mathcal{I}G_A\mathcal{I} = \mathcal{I}_A G_A \mathcal{I}_A = \begin{pmatrix} G_A & 0 \\ 0 & 0 \end{pmatrix}, \qquad \mathcal{G}_A^{-1} = \begin{pmatrix} G_A^{-1} & 0 \\ 0 & 0 \end{pmatrix}, \tag{7.5}$$

and $\mathcal{G}_A\mathcal{G}_A^{-1}$ is just $\mathcal{I}_A$.

7.1. *The matched Green function G_s*

Let us indicate now points on the A/B side by $\boldsymbol{R}_A$ and $\boldsymbol{R}_B$, respectively. An elementary excitation in the whole system can either propagate directly from $\boldsymbol{R}'_B$ to $\boldsymbol{R}_B$, both within P_B or else propagate to the interface domain $\mathcal{I}$, and there: (a) undergo a reflection, described by some surface object $\mathcal{R} = \mathcal{I}R\mathcal{I} = \mathcal{I}_B R \mathcal{I}_B$, and then propagate to $\boldsymbol{R}_B$; (b) undergo a transmission described by some surface object $\mathcal{T} = \mathcal{I}T\mathcal{I} = \mathcal{I}_A T \mathcal{I}_B$, and then propagate to $\boldsymbol{R}_A$, as indicated in fig. 10.

The two distinctly different projections of G_s are now

$$P_B G_s P_B = P_B G_B P_B + P_B G_B \mathcal{R} G_B P_B , \qquad P_A G_s P_B = P_A G_A \mathcal{T} G_B P_B . \tag{7.6}$$

Projecting onto the appropriate domains $\mathcal{I}_M$ one finds

$$\mathcal{T} = \mathcal{G}_A^{-1} \mathcal{G}_s \mathcal{G}_B^{-1} , \qquad \mathcal{R} = \mathcal{G}_B^{-1} (\mathcal{G}_s - \mathcal{G}_B) \mathcal{G}_B^{-1} , \tag{7.7}$$

whence the transmission and reflection scattering amplitudes

$$f_T = \mathcal{I}_A \mathcal{G}_s \mathcal{G}_B^{-1} , \qquad f_R = \mathcal{I}_B (\mathcal{G}_s - \mathcal{G}_B^{-1}) \mathcal{G}_B^{-1} , \tag{7.8}$$

and the formulae [compare with (2.4, 2.5), where the sides A and B coalesce into the plane $z = 0$]

$$\begin{aligned} P_B G_s P_B &= P_B G_B P_B + P_B G_B \mathcal{G}_B^{-1} (\mathcal{G}_s - \mathcal{G}_B) \mathcal{G}_B^{-1} G_B P_B , \\ P_A G_s P_B &= P_A G_A \mathcal{G}_A^{-1} \mathcal{G}_s \mathcal{G}_B^{-1} G_B P_B . \end{aligned} \tag{7.9}$$

One could equally start from side A and obtain the dual formulae with A and B interchanged. Let here and henceforth $\bar{M}$ indicate the *other* side, that is B/A if M is A/B. Taking $\mathcal{I}_M$ $(M' = M, \bar{M})$ projections from the right or from the left,

$$P_M G_s \mathcal{I}_{M'} = P_M G_M \mathcal{G}_M^{-1} \mathcal{G}_s \mathcal{I}_{M'} , \qquad \mathcal{I}_{M'} G_s P_M = I_{M'} \mathcal{G}_s \mathcal{G}_M^{-1} G_M P_M , \tag{7.10}$$

and, adding up for the two values of M' $(M, \bar{M})$ we have, quite generally

$$P_M G_s \mathcal{I} = P_M G_M \mathcal{G}_M^{-1} \mathcal{G}_s \mathcal{I} , \qquad \mathcal{I} G_s P_M = \mathcal{I} \mathcal{G}_s \mathcal{G}_M^{-1} G_M P_M . \tag{7.11}$$

These formulae have the same form as those originally derived for continuous media [2], but they contain an important element in an atomistic description of discrete media. Every G_M is only used in the space in which it is meaningful. For example, matrix elements of H_A or G_A between atomic states of B atoms would never enter this analysis.

The local density of states (LDOS) in the successive layers on either side, for fixed κ, is given by

$$N_n(\kappa, \Omega) = -\frac{1}{\pi} \operatorname{Im} \operatorname{Tr} \langle n | G_s(\Omega^+) | n \rangle , \quad \Omega^+ = \Omega + i\varepsilon , \quad \varepsilon \to 0 , \tag{7.12}$$

with G_s taken from either the P_A or the P_B domain.

7.2. *The matching formula*

To obtain the formula for $\mathcal{G}_s$ we start from eqs. (7.2) and (7.3) and project onto $\mathcal{I} = \mathcal{I}_A + \mathcal{I}_B$ (fig. 10), which yields

$$\Omega \mathcal{G}_s - \mathcal{I} H_s (P_A + P_B) G_s \mathcal{I} = \mathcal{I} . \tag{7.13}$$

Using eq. (7.11) again for each $P_M G_s \mathcal{I}$ term in eq. (7.13) one finds the new matching formula for an arbitrary interface

$$\mathcal{G}^{-1} = \Omega\mathcal{I} - \mathcal{I}H_s P_A \mathcal{G}_A^{-1} - \mathcal{I}H_s P_B \mathcal{G}_B^{-1} . \tag{7.14}$$

The terms (matrix elements in an explicit representation) entering this formula have an obvious meaning: $I_M H_s P_M$ includes interactions between boundary-M atoms and any M atoms. $\mathcal{I}_{\bar{M}} H_s P_M$, which is just $\mathcal{I}_{\bar{M}} H_s \mathcal{I}_M$, contains the $\bar{M}M$ coupling at the interface. The precise specification of these terms constitutes the model for the interface and

$$\det|\mathcal{G}_s^{-1}| = 0 \tag{7.15}$$

is the secular equation for the (matching) interface states. We can now define arbitrarily the ideal *interface* as that in which the coupling terms exist but where on each side $P_M H_s P_M$ is just the unperturbed $P_M H_M P_M$. The *interface perturbation* is then defined as

$$V_s = \mathcal{I}_A(\Delta H_A)\mathcal{I}_A + \mathcal{I}_B(\Delta H_B)\mathcal{I}_B \tag{7.16}$$

and then eq. (7.14) becomes

$$\mathcal{G}_s^{-1} = \mathcal{G}_{s0}^{-1} - V_s . \tag{7.17}$$

From a practical point of view it is interesting to note that

$$\begin{aligned}\mathcal{G}_s^{-1} = {} & (\mathcal{I}_A \Omega \mathcal{I}_A - \mathcal{I}_A H_A P_A G_A \mathcal{G}_A^{-1} \mathcal{I}_A) + (\mathcal{I}_B \Omega \mathcal{I}_B - \mathcal{I}_B H_B P_B G_B \mathcal{G}_B^{-1} \mathcal{I}_B) \\ & - (\mathcal{I}_A H_s \mathcal{I}_B + \mathcal{I}_B H_s \mathcal{I}_A) .\end{aligned} \tag{7.18}$$

The point is that the first two terms have often been studied separately. Each one gives the free surface matching formula for each M. Thus the work done to study each incomplete crystal separately can be directly used to study the coupled, and eventually perturbed, interface. Note that the secular equation based on eq. (7.17) contains no redundant information.

This analysis differs from other Green function treatments of the interface problems [79] in which the secular determinant is larger than necessary and the roots corresponding to each separate semi-infinite crystal must be sorted out in order to be left with the interface states. The above results hold for an interface of arbitrary shape and can equally be applied to study localised defects like substitutional or interstitial impurities [43].

After this formal presentation of the SGFM method for the single interface case we shall illustrate how the method works in practice by presenting some interface electronic structure calculations with empirical tight-binding (ETB) models. We shall consider the (001) Ge–GaAs heterojunctions. In this case one *layer* will contain two atomic planes, because we consider second-nearest-neighbour interactions, and we shall use a four-states basis, namely one with one s and three p orbitals.

Let us indicate by $\mathcal{I}_n$ the projector or unit matrix of layer n. Consequently the Hamiltonian "matrix elements", written as $\mathcal{I}_n H \mathcal{I}_{n'}$ or $H_{n,n'}$, indiscriminately, according to convenience, will be $\boldsymbol{\kappa}$-dependent 8×8 matrices. The same applies to the Green function "matrix elements" $\mathcal{I}_n G \mathcal{I}_{n'}$ or $G_{nn'}$, which are $\boldsymbol{\kappa}$- and energy-dependent 8×8 matrices.

The structure of the secular matrix is actually very simple. Assume, for instance, A on the left and B on the right and concentrate on

$$\mathcal{G}_{s,B}^{-1} = \mathcal{I}_B E \mathcal{I}_B - \mathcal{I}_B H_B P_B G_B \mathcal{G}_B^{-1} . \tag{7.19}$$

Let $n = 1$ correspond to $\mathcal{I}_B$. Then, by definition of the principal layer

$$\mathcal{I}_B H_B P_B = H_{B,11} + H_{B,12} , \qquad \mathcal{G}_B = G_{B,11} \tag{7.20}$$

and

$$\mathcal{G}_{s,B}^{-1} = (E - H_B)_{11} - H_{B,12} T_B , \tag{7.21}$$

where

$$T_B = G_{B,21} G_{B,11}^{-1} \tag{7.22}$$

is the transfer matrix for the bulk crystal B. More about the practical advantages for computation of the transfer matrices will be presented in section 9. Here and in the following we shall give the main formulae in terms of transfer matrices where they are convenient. Note that T_B is defined by eq. (7.22) and corresponds to a displacement of the *first* layer index, from $G_{n,n}$ to $G_{n+1,n}$, that is to the right. The same applies to the A side but changing right into left. Additional transfer matrices appearing in later formulae are defined by

$$G_{B,01} = \bar{T}_B G_{B,11} , \qquad G_{B,12} = G_{B,11} S_B , \qquad G_{B,10} = G_{B,11} \bar{S}_B , \tag{7.23}$$

and analogous expressions for crystal A.

The first layer on going into A corresponds to $n = 0$ and

$$T_A = G_{A,-10} G_{A,00}^{-1} . \tag{7.24}$$

Thus

$$\mathcal{G}_s^{-1} = [(E - H_A)_{00} - H_{A,0-1} T_A] + [(E - H_B)_{11} - H_{B,12} T_B] - [H_{1,10} + H_{1,01}] . \tag{7.25}$$

This involves only Hamiltonian matrix elements and T, which can also be evaluated by matrix algebra involving only Hamiltonian matrix elements as will be seen later. Thus the secular matrix involves only Hamiltonian matrix elements. It does not even require the knowledge of the bulk Green functions. Moreover, eq. (7.25) used directly the information on semi-infinite A, semi-infinite B and cross coupling. The secular equation (7.15) is only a 2×2 supermatrix and it contains no redundant information. Every root of the secular equation is an eigenvalue of the interface problem. The structure of the secular matrix is very simple indeed. In practice the interface states can alternatively be obtained from the singularities of the imaginary part of Tr $\mathcal{G}_s$. In fact this is a practical method, and describes equally well resonances and similar solutions. Indeed, the trace of $\mathcal{G}_s$ is just what one needs to calculate the density of states in the interface layers, that is

$$N_s(\kappa, E) = -\frac{1}{\pi} \lim_{\varepsilon \to 0} \operatorname{Im} \operatorname{Tr} \mathcal{G}_s(\kappa, E + i\varepsilon) . \tag{7.26}$$

In the present example this involves a sum over four atomic planes and each one contributes the trace of a 4×4 submatrix corresponding to the four basis states. The contribution of each atomic plane can be separately identified. The SGFM analysis yields the formula for all matrix elements of G_s in terms of its own projection $\mathcal{G}_s$ as explained before. From the diagonal terms we calculate the LDOS in any desired layer n. For example, on the B side

$$G_{s,nn} = G_{B,nn} + G_{B,n1} G^{-1}_{B,11} (G_{s,11} - G_{B,11}) G^{-1}_{B,11} G_{B,1n} , \tag{7.27}$$

where $G_{s,11}$ is the projection of G_s on the $\mathcal{S}_B$ domain ($n = 1$). Then, for side B, we have

$$G_{s,nn} = G_{B,11} + T^n_B (G_{s,11} - G_{B,11}) S^n_B . \tag{7.28}$$

Note that this is an explicit formula, not a recurrence relation. At this stage the matrix G_{11} is needed. However, if one knows the transfer matrices then G_{11} can be evaluated by simple matrix algebra as will be seen later. As explained before G_s can be employed both to obtain the band structure of the interface and to calculate the LDOS for the atomic planes within the interface domain. Beyond these the LDOS must be calculated from eq. (7.28).

Ideal [44] and non-ideal [45] Ge–GaAs (001) interfaces have been calculated with this method by using the ETB Hamiltonian of Chadi [80] for the bulk materials, and taking the arithmetic averages of the corresponding bulk parameters for the cross-coupling matrix elements. As an illustration we show in figs. 11 and 12 the LDOS summed over the two-dimensional Brillouin zone for the first four atomic

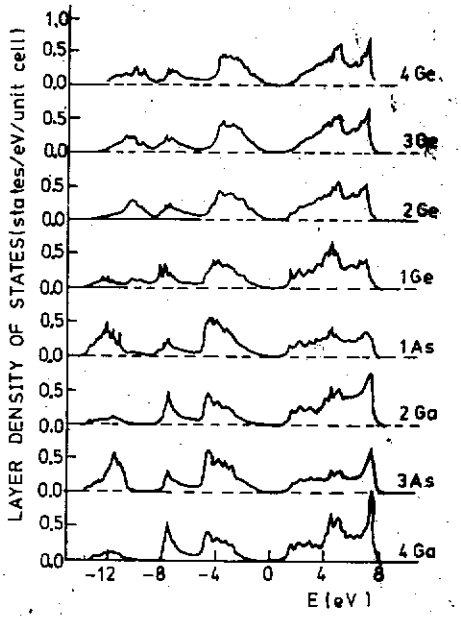

Fig. 11. LDOS integrated over the two-dimensional Brillouin zone, for the first four atomic planes on each side of the ideal (001) Ge–Ga interface, with a valence-band discontinuity of 0.9 eV.

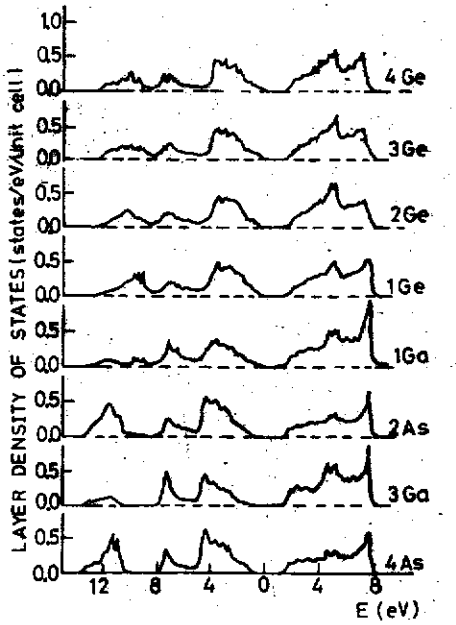

Fig. 12. As in fig. 12, for the ideal (001) Ge–As interface.

planes on each side of the ideal (001) Ge–Ga and Ge–As interfaces, using a valence-band discontinuity of 0.9 eV. Both figures show that the interface-induced effects are mainly restricted to the two atomic planes forming the geometrical interface. No separate interface states are present in the gap regions, and there are only small changes within the band continuum.

This method has also been applied to the study of phonons at the (001) interface of BCC transition metals [81].

8. Discrete media: multiple interfaces

Having seen the case of a single interface, we now discuss multiple interfaces. As prime examples of widespread physical interest we concentrate on quantum wells and superlattices again.

8.1. *The sandwich or quantum well structure*

The system is sketched in fig. 13, where l, m and r indicate left, middle and right, respectively. The corresponding media have Green functions G_M and projectors P_M, with $M = l, m, r$. Now we have two interfaces, one on the left (l) and the other one on the right (r). Let us indicate by $\mathcal{I}_l$ and $\mathcal{I}_r$, fig. 13, the corresponding projectors of the said interface domain. Each one has two subdomains, as in section 7, and in each one the corresponding surface object, with its inverse, is defined. Now, however, $\mathcal{G}_l$ and $\mathcal{G}_r$ are seen as 2×2 supermatrices with only one full box, in the space of the l- and r-interfaces, respectively, that is

$$\mathcal{I}_l\mathcal{G}_l\mathcal{I}_l = (\mathcal{I}_{ll}+\mathcal{I}_{lm})\mathcal{G}_l(\mathcal{I}_{ll}+\mathcal{I}_{lm}) = \mathcal{I}_{ll}\mathcal{G}_l\mathcal{I}_{ll} = \begin{pmatrix} \mathcal{G}_l & 0 \\ 0 & 0 \end{pmatrix},$$
$$\mathcal{I}_r\mathcal{G}_r\mathcal{I}_r = (\mathcal{I}_{rr}+\mathcal{I}_{rm})\mathcal{G}_r(\mathcal{I}_{rr}+\mathcal{I}_{rm}) = \mathcal{I}_{rr}\mathcal{G}_r\mathcal{I}_{rr} = \begin{pmatrix} 0 & 0 \\ 0 & \mathcal{G}_r \end{pmatrix}. \tag{8.1}$$

Then

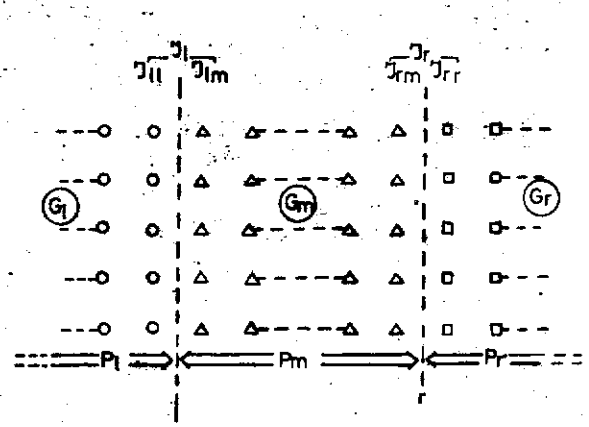

Fig. 13. A sandwich-type structure. For electronic states, with $G_l = G_r$, this is the quantum well. Note the structure of the interface domains in the subdomains.

$$\mathcal{I}_l \mathcal{G}_l^{-1} \mathcal{I}_l = \begin{pmatrix} \mathcal{G}_l^{-1} & 0 \\ 0 & 0 \end{pmatrix}, \qquad \mathcal{I}_l \mathcal{G}_l^{-1} \mathcal{G}_l \mathcal{I}_l = \begin{pmatrix} I_{ll} & 0 \\ 0 & 0 \end{pmatrix}, \tag{8.2}$$

and one never performs an illegitimate matrix inversion. In the present case there are two, generally coupled, interfaces and the projection domain, where all the physics of the problem is contained, consists of $\mathcal{I}_l$ and $\mathcal{I}_r$. Thus the entire interface domain will be defined as consisting of both l and r and having the projector

$$\mathcal{I} = \mathcal{I}_l + \mathcal{I}_r = \mathcal{I}_{ll} + \mathcal{I}_{lm} + \mathcal{I}_{rm} + \mathcal{I}_{rr} . \tag{8.3}$$

Considered in this space all surface objects become (4×4) supermatrices. Again one must note which boxes are empty and how inverses are defined. Thus eqs. (8.1) and (8.2) become

$$\mathcal{I}\mathcal{G}\mathcal{I} = \begin{pmatrix} \mathcal{G}_l & 0 & 0 & 0 \\ 0 & 0 & 0 & 0 \\ 0 & 0 & 0 & 0 \\ 0 & 0 & 0 & 0 \end{pmatrix}, \qquad \mathcal{I}\mathcal{G}_l \mathcal{G}_l^{-1} \mathcal{I} = \begin{pmatrix} I_{ll} & 0 & 0 & 0 \\ 0 & 0 & 0 & 0 \\ 0 & 0 & 0 & 0 \\ 0 & 0 & 0 & 0 \end{pmatrix}. \tag{8.4}$$

The definition of the projection is different for G_m because it is through the cross matrix elements of G_m between l and r that the coupling between the two interfaces enters the problem. The appropriate definition is then $\tilde{G}_m = (\mathcal{I}_{lm} + \mathcal{I}_{rm}) G_m (\mathcal{I}_{lm} + \mathcal{I}_{rm})$, which considered in the entire interface domain $\mathcal{I}$ is

$$\tilde{G}_m = \mathcal{I} G_m \mathcal{I} = \begin{pmatrix} 0 & 0 & 0 & 0 \\ 0 & \mathcal{I}_{lm} G_m \mathcal{I}_{lm} & \mathcal{I}_{lm} G_m \mathcal{I}_{rm} & 0 \\ 0 & \mathcal{I}_{rm} G_m \mathcal{I}_{lm} & \mathcal{I}_{rm} G_m \mathcal{I}_{rm} & 0 \\ 0 & 0 & 0 & 0 \end{pmatrix}, \tag{8.5}$$

displaying again which boxes of the 4×4 supermatrix are empty. The physical reason is again the same. Matrix elements of G_m between states of l or r atoms are meaningless. Note that $\tilde{G}_m$ is actually first defined in its own space, $\mathcal{I}_{lm} + \mathcal{I}_{rm}$, and then considered in $\mathcal{I}$. The inverse $\tilde{G}_m^{-1}$ is defined by observing the same rule. One first defines the inverse of the matrix $(\mathcal{I}_{lm} + \mathcal{I}_{rm}) G_m (\mathcal{I}_{lm} + \mathcal{I}_{rm})$, that is the central 2×2 supermatrix contained in the larger 4×4 supermatrix of eq. (8.5), so that

$$\tilde{G}_m^{-1} \tilde{G}_m = (\mathcal{I}_{lm} + \mathcal{I}_{rm}) \tilde{G}_m^{-1} \tilde{G}_m (\mathcal{I}_{lm} + \mathcal{I}_{rm}) = \begin{pmatrix} I_{lm} & 0 \\ 0 & I_{rm} \end{pmatrix}, \tag{8.6}$$

and then $\tilde{G}_m^{-1}$ again becomes the central block in a 4×4 supermatrix like (8.5) so that

$$\mathcal{I} \tilde{G}_m^{-1} \tilde{G}_m \mathcal{I} = \begin{pmatrix} 0 & 0 & 0 & 0 \\ 0 & I_{lm} & 0 & 0 \\ 0 & 0 & I_{rm} & 0 \\ 0 & 0 & 0 & 0 \end{pmatrix}. \tag{8.7}$$

The surface objects thus defined will now play their usual role in the SGFM analysis, which is then set up as follows. First one must choose a model and define the "Hamiltonian", of the system. Physically one has the l, m and r crystalline media in their respective domains, their possible perturbations in the interface domains and their coupling interactions across the interfaces. We shall indicate the bulk

"Hamiltonians" by H_M $(M = l, m, r)$. By definition the interface domains include all atoms – or layers – that are affected by the creation of interfaces. Thus the possible perturbations ΔH_M are localized within the corresponding subdomains, for example, $\mathcal{I}_{ll}\,\Delta H_l \mathcal{I}_{ll}$ and the coupling terms are likewise localised. The "Hamiltonian" of the system under study is then

$$H_s = P_l H_l P_l + P_m H_m P_m + P_r H_r P_r + \mathcal{I}\,\Delta H \mathcal{I} + \mathcal{I} H^{\times} \mathcal{I}\,, \tag{8.8}$$

where

$$\begin{aligned} \mathcal{I}\,\Delta H \mathcal{I} &= \mathcal{I}_{ll}\,\Delta H_l \mathcal{I}_{ll} + \mathcal{I}_{lm}\,\Delta H_m \mathcal{I}_{lm} + \mathcal{I}_{rm}\,\Delta H_m \mathcal{I}_{rm} + \mathcal{I}_{rr}\,\Delta H_r \mathcal{I}_{rr}\,, \\ \mathcal{I} H^{\times} \mathcal{I} &= \mathcal{I}_{ll} H^{\times} \mathcal{I}_{lm} + \mathcal{I}_{lm} H^{\times} \mathcal{I}_{ll} + \mathcal{I}_{rm} H^{\times} \mathcal{I}_{rr} + \mathcal{I}_{rr} H^{\times} \mathcal{I}_{rm}\,. \end{aligned} \tag{8.9}$$

The first three terms of (8.8) represent the ideally truncated l-, m- and r-parts. The fourth term represents the local changes affecting the boundary atoms and the last one embodies the $l - m$ and $m - r$ couplings at the respective interfaces.

The model contains all the information put into eq. (8.8). Once this has been defined, the form of the relationship between G_s and its own projection $\tilde{G}_s$ is the same as in the continuous case. This part of the SGFM analysis proceeds in exactly the same way, only that the continuous position variable z is replaced by the discrete layer index n. This can be conveniently cast in terms of the projectors P_l, P_m and P_r. For instance, when both n and n' are in the domain of P_m, then

$$P_m G_s P_m = P_m G_m P_m + P_m G_m \tilde{G}_m^{-1} (\tilde{G}_s - \tilde{G}_m) \tilde{G}_m^{-1} G_m P_m\,. \tag{8.10}$$

Note that $\tilde{G}_s$ is defined like $\tilde{G}_m$ in (8.5), but all its boxes are full. Now define the external projector P_e and external resolvent G_e

$$P_e = P_l + P_r\,, \qquad G_e = P_e G_e P_e = P_l G_l P_l + P_r G_r P_r\,, \tag{8.11}$$

so that the complete surface projection of G_e is

$$\tilde{G}_e = \mathcal{I} G_e \mathcal{I} = \mathcal{I}_l G_l \mathcal{I}_l + \mathcal{I}_r G_r \mathcal{I}_r = \begin{pmatrix} \mathcal{I}_{ll} G_l \mathcal{I}_{ll} & 0 & 0 & 0 \\ 0 & 0 & 0 & 0 \\ 0 & 0 & 0 & 0 \\ 0 & 0 & 0 & \mathcal{I}_{rr} G_r \mathcal{I}_{rr} \end{pmatrix}, \tag{8.12}$$

and its inverse is

$$\tilde{G}_e^{-1} = \begin{pmatrix} \mathcal{I}_{ll} G_l^{-1} \mathcal{I}_{ll} & 0 & 0 & 0 \\ 0 & 0 & 0 & 0 \\ 0 & 0 & 0 & 0 \\ 0 & 0 & 0 & \mathcal{I}_{rr} G_r^{-1} \mathcal{I}_{rr} \end{pmatrix}. \tag{8.13}$$

Then

$$P_e G_s P_m = P_e G_e \tilde{G}_e^{-1} \tilde{G}_s \tilde{G}_m^{-1} G_m P_m\,. \tag{8.14}$$

The matrix elements $P_m G_s P_m^*$, eq. (8.10), and $P_e G_s P_m$, eq. (8.14), are identical in form to the $P_B G_s P_B$ and $P_A G_s P_B$ matrix elements for the one-interface problem, eq. (7.6), with in/out replacing the B/A sides and hence 4×4 supermatrices appearing instead of the 2×2 supermatrices of the one-interface case.

It only remains to give the matching formula for $\tilde{G}_s$, which can be done by starting from the equation of motion

$$(\Omega - H_s)G_s = P_e + P_m\,, \tag{8.15}$$

taking appropriate projections and using eqs. (8.10) and (8.14). In fact from this point on there is complete isomorphism between this problem and the one-interface problem studied before, and the analysis consists of a mere formal repetition of the steps taken in the former section. It can be easily seen that

$$\tilde{G}_s^{-1} = \Omega\mathcal{I} - \mathcal{I}H_s(P_e G_e \tilde{G}_e^{-1} + P_m G_m \tilde{G}_m^{-1})\,. \tag{8.16}$$

Knowing $\tilde{G}_s$ one knows the complete G_s and one has the complete physics of the problem at hand in the usual way. In particular, the secular equation for the matching states is

$$\det|\tilde{G}_s^{-1}(\kappa, \Omega)| = 0\,, \tag{8.17}$$

where we have Fourier transformed in the planes of the interfaces and the matching states will have amplitudes localized near $\mathcal{I}_l$ and $\mathcal{I}_r$. Their local spectral strength is obtained from the diagonal parts $P_m G_s P_m$, eq. (8.10), and $P_e G_s P_e$, which is analogously obtained as

$$P_e G_s P_e = P_e G_e P_e + P_e G_e \tilde{G}_e^{-1}(\tilde{G}_s - \tilde{G}_e)\tilde{G}_e^{-1} G_e P_e\,. \tag{8.18}$$

Both equations (8.10) and (8.18) are also Fourier transformed so that from the imaginary part of the local trace projected on a given atomic plane we can obtain the LDOS for given κ. Any other spectral function of interest can be obtained again by starting from here.

8.2. The superlattice

Consider now a superlattice . . . A–B–A–B . . .. The situation is sketched in fig. 14, which displays the distinct features of the discrete case. Here m and n denote another two interfaces and d is the length of the period. This entails a phase factor $f = \exp(i\eta)$, where $\eta = qd$, for states with (super)momentum q associated with the superperiodicity of period d.

The structure of all the terms concerning the interfaces follows from an analysis identical to that of the earlier section. It is now convenient to define surface objects and projections as before, with appropriate modifications. In order to indicate projections on the two coupled interfaces limiting a slab of material A, the definitions of $\tilde{G}_m$ and $\tilde{G}_s$ now become

$$\tilde{G}_A = (\mathcal{I}_l + \mathcal{I}_r)G_A(\mathcal{I}_l + \mathcal{I}_r)\,, \qquad \tilde{G}_{sA} = (\mathcal{I}_l + \mathcal{I}_r)G_s(\mathcal{I}_l + \mathcal{I}_r)\,. \tag{8.19}$$

Again, one must keep in mind details like the fact that out of, for example, $\mathcal{I}_l G_A \mathcal{I}_l$ only the $\mathcal{I}_{lA} G_A \mathcal{I}_{lA}$

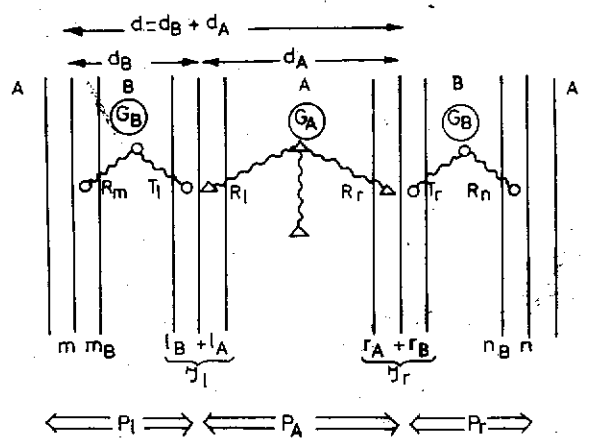

Fig. 14. Same as fig. 3, with atomic structure and interface domains and subdomains, for the superlattice ... A–B–A–B ....

has non-vanishing boxes in the 4×4 supermatrix format, etc. The algebra of subsection 8.1 can then be repeated with the conspicuous difference that the P_l and P_r domains are now finite, which brings in two extra terms involving the phase factor f. The diagonal terms inside P_A are now compacted into [42, 43]

$$P_A G_s P_A = P_A G_A P_A + P_A G_A \tilde{G}_A^{-1} (\tilde{G}_{sA} - \tilde{G}_A) \tilde{G}_A^{-1} G_A P_A . \tag{8.20}$$

The sum of the cross terms is more involved. It is now convenient to define the projector

$$\hat{P} = P_l + P_r \tag{8.21}$$

and, cast in the 2×2 format,

$$\hat{P} G_{\beta\eta} I = \begin{pmatrix} P_l G_B \mathcal{J}_l & \exp(-i\eta) P_l G_B \mathcal{J}_m \\ \exp(i\eta) P_r G_B \mathcal{J}_n & P_r G_B \mathcal{J}_r \end{pmatrix}, \tag{8.22a}$$

$$\hat{G}_{\beta\eta} = \begin{pmatrix} \mathcal{J}_l G_B \mathcal{J}_l & \exp(-i\eta) \mathcal{J}_l G_B \mathcal{J}_m \\ \exp(i\eta) \mathcal{J}_r G_B \mathcal{J}_n & \mathcal{J}_r G_B \mathcal{J}_r \end{pmatrix}. \tag{8.22b}$$

Note that all the information is now folded into the supermatrix referred to l and r. Thus a term like $\mathcal{J}_l G_B \mathcal{J}_m$ occupies the place labelled (l, r) but it carries the corresponding phase factor. After some algebra [42, 43] one has the new matching formula

$$\tilde{G}_{sA}^{-1} = \Omega \mathcal{J} - \mathcal{J} H_s (\hat{P} G_{\beta\eta} \hat{G}_{\beta\eta}^{-1} + P_A G_A \tilde{G}_A^{-1}) . \tag{8.23}$$

There is an important difference between this and eq. (8.16) in that, after appropriate Fourier transformation, eq. (8.16) is a function of (κ, Ω), whereas (8.23) is a function of (κ, q, Ω). Thus the new secular equation,

(8.24)

yields the new band structure of the superlattice, and this includes the effect of the superperiodicity through q and that of the possible κ-dependent bands of matching states. The spectral functions of interest are obtained from the diagonal part, eq. (8.20). The momentum variable q is canonically conjugate to the *superlattice* position coordinate, measured in multiples of d, and *not* to the lattice position coordinate contained in P_A. Thus from the trace of the imaginary part of eq. (8.20) one obtains directly the density of states in the slabs of material A for given κ and q.

The analysis presented until now has focused on the two interfaces limiting a slab of material A. Of course, the dual choice is equally legitimate and the same formulae hold *mutatis mutandis* if one takes the projection on two consecutive interfaces limiting a slab of material B. Hence one has at once a formula for $\tilde{G}_{sB}$ instead of $\tilde{G}_{sA}$, which provides an alternative expression for the secular equation and from which $P_B G_s P_B$ is obtained at once by interchanging A and B in eq. (8.23). Let us now see the practical implementation of these formulae.

The elements of the Green functions can be conveniently obtained by using the transfer matrices introduced previously.

The SGFM formulae needed for actual calculations are then cast in the following form:

$$\tilde{G}_{sA}^{-1} = \begin{pmatrix} (ll) & (lr) \\ (rl) & (rr) \end{pmatrix}, \tag{8.25}$$

where

$$(ll) = \begin{pmatrix} l_B(E - H_s)H_B - l_B D_B L_B & -l_B H_i l_A \\ -l_A H_i l_B & l_A(E - H_s)l_A - l_A D_A l_A \end{pmatrix},$$

$$(lr) = \begin{pmatrix} 0 & -l_B D_B r_B \\ -l_A D_A r_A & 0 \end{pmatrix}, \quad (rl) = \begin{pmatrix} 0 & -r_A D_A l_A \\ -r_B D_B l_B & 0 \end{pmatrix},$$

$$(rr) = \begin{pmatrix} r_A(E - H_s)r_A - r_A D_A r_A & -r_A H_i r_B \\ -r_B H_i r_A & r_B(E - H_s)r_B - r_B D_B r_B \end{pmatrix},$$

and

$$\begin{pmatrix} l_A D_A l_A & l_A D_A r_A \\ r_A D_A l_A & r_A D_A r_A \end{pmatrix} = \begin{pmatrix} H_A(1,2) & 0 \\ 0 & H_A(2,1) \end{pmatrix} \rho_A \tau_A^{-1}, \tag{8.26}$$

$$\begin{pmatrix} l_B D_B l_B & l_B D_B r_B \\ r_B D_B l_B & r_B D_B r_B \end{pmatrix} = \begin{pmatrix} H_B(2,1) & 0 \\ 0 & H_B(1,2) \end{pmatrix} \rho_B \tau_B^{-1}, \tag{8.27}$$

$$\rho_A = \begin{pmatrix} T_A & \bar{T}_A^{(\nu_A - 1)} \\ T_A^{(\nu_A - 1)} & \bar{T}_A \end{pmatrix}, \quad \tau_A = \begin{pmatrix} I_A & \bar{T}_A^{-\nu_A} \\ T_A^{\nu_A} & I_A \end{pmatrix}, \tag{8.28}$$

$$\rho_B = \begin{pmatrix} \bar{T}_B & f^{-1} T_B^{(\nu_B - 1)} \\ f\bar{T}_B^{(\nu_B - 1)} & T_B \end{pmatrix}, \quad \tau_B = \begin{pmatrix} I_B & f^{-1} T_B^{\nu_B} \\ f\bar{T}_B^{\nu_B} & I_B \end{pmatrix}. \tag{8.29}$$

The local spectral strength in the layer n_A is obtained from

$$G_s(n_A, n_A) = \mathcal{G}_A + (T_A^{(n_A-1)}, \bar{T}_A^{(\nu_A+1-n_A)}) \cdot \mu_A \cdot \begin{pmatrix} S_A^{(n_A-1)} \\ \bar{S}_A^{(\nu_A+1-n_A)} \end{pmatrix}, \tag{8.30}$$

$$\mathcal{J}_A \mu_A \mathcal{J}_A \equiv \mu_A = \tau_A^{-1}(\mathcal{J}_A \tilde{G}_{sA} \mathcal{J}_A - \tilde{g}_A)\sigma_A^{-1}, \tag{8.31}$$

$$\tilde{g}_A = \begin{pmatrix} \mathcal{G}_A & 0 \\ 0 & \mathcal{G}_A \end{pmatrix}, \quad \mathcal{G}_A = G_A(n_A, n_A), \quad \sigma_A = \begin{pmatrix} I_A & S_A^{\nu_A} \\ \bar{S}_A^{\nu_A} & I_A \end{pmatrix}, \tag{8.32}$$

and the dual formulae with the roles of A and B interchanged.

The labelling of the layers and the meanings of ν_A and ν_B are shown in fig. 15. In order to obtain the LDOS for given κ we must integrate over q, the perpendicular component of the wavevector. The above formulae cannot be literally applied to the particular case in which one of the slabs is reduced to just one layer. This is the situation for periodic intercalation compounds but the same method can be readily adapted to this case [49]. Note that one *layer* may, and usually does, contain more than one atomic layer. The LDOS is obtained from the trace of $G_s(n, n)$ and this sums over the atomic layers forming the *layer* n. The separate contributions from each atomic layer yield the corresponding local spectral strengths.

Now having calculated the LDOS in the A layers, the question is how to do the same for the B layers. The straightforward way would seem to be to resort to the set of dual formulae, with A and B and their roles interchanged. This would obviously be correct, but impracticable, because the projections are then not in the domain (l, r) but in, say, (r, n). $\tilde{G}_{sB}$, for instance, is not the same matrix as $\tilde{G}_{s,A}$, although both yield the same secular determinant. A parallel calculation of the dual formulae requires a recalculation of the secular matrix and Green function elements, which would be highly redundant as all the physical information should be contained in the projection on (l, r). An alternative formulation for the B part, whose formal aspects need not be given here, can be obtained and it has considerable practical advantages concerning both memory requirements and computer time, against the dual formulae for B. This yields the following expression for the local spectral strength in an n_B layer:

$$G_s(n_B, n_B) = \mathcal{G}_B + (\bar{T}_B^{n_B-1}, f^{-1}T_B^{(\nu_B+1-n_B)})\mu_B \begin{pmatrix} \bar{S}_B^{(n_B-1)} \\ fS_B^{(\nu_B+1-n_B)} \end{pmatrix}, \tag{8.33}$$

where

$$\mu_B = \tau^{-1}(\tilde{G}_{sA} - \tilde{g}_B)\sigma_B^{-1}, \tag{8.34}$$

$$\tilde{g}_B = \begin{pmatrix} \mathcal{G}_B & 0 \\ 0 & \mathcal{G}_B \end{pmatrix}, \quad \mathcal{G}_B = G_B(n_B, n_B), \quad \sigma_B = \begin{pmatrix} I_B & f^{-1}\bar{S}_B^{\nu_B} \\ fS_B^{\nu_B} & I_B \end{pmatrix}. \tag{8.35}$$

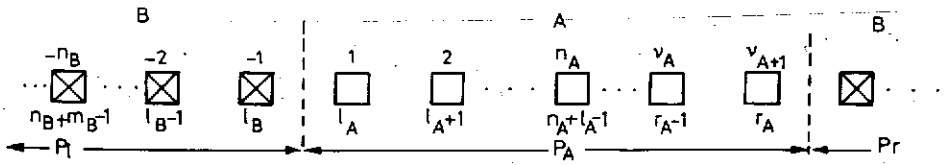

Fig. 15. The ordering and labelling of the different layers of the superlattice. Each square represents a principal layer.

Now the same type of calculation and the same projections are employed for the A and B parts of the superlattice in such a way that no redundant calculations must be performed.

The above formulae are prepared so that once the transfer matrices are evaluated they are directly inserted in the algebra yielding the secular matrix and then the diagonal-layer projections. Altogether this provides a very efficient computational procedure. It is important to stress that in this method the dimension of the secular determinant is only fixed by the size of the basis and the range of the interactions, but not by the period of the superlattice. In the case of nearest-neighbour interactions and a sp^3s^* basis the secular matrix (8.25) is 40×40 [51], whereas for a force constant model for transition metals including central interactions up to third nearest neighbours and angular interactions up to second nearest neighbours [50] the secular matrix (8.25) is 24×24. The increase of the superlattice period is reflected in this method in the need to calculate higher powers in the σ-, τ- and ρ-matrices in the A and B parts.

In practical calculations the band structure can be obtained either by looking for the zeros of (8.25) or for peaks in the local spectral strength given by eqs. (8.30) and (8.33). As in the case of superlattices one is also interested in the spatial localization or confinement of the different modes and this can be

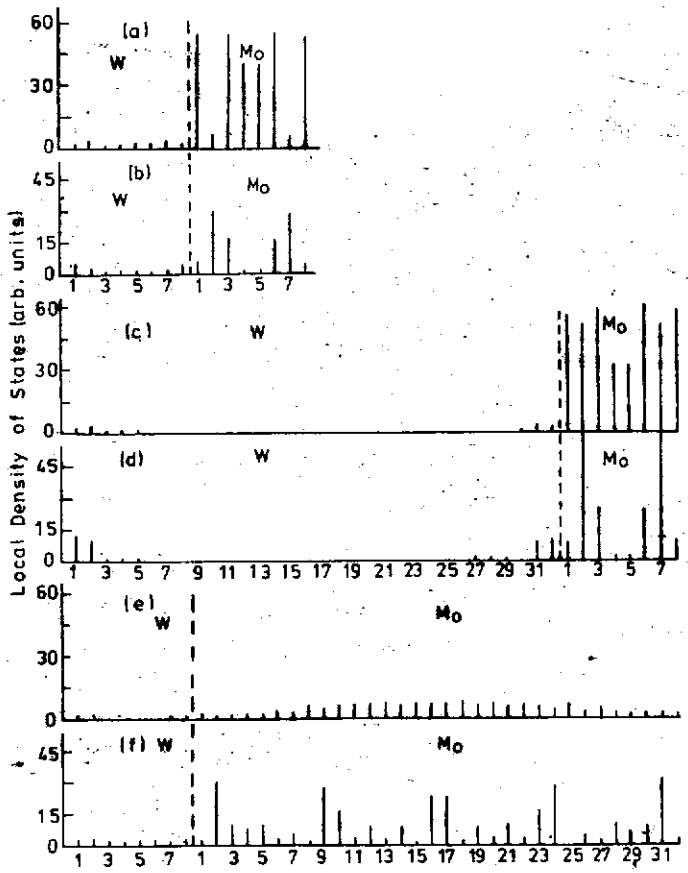

Fig. 16. Local spectral strength at the different atomic layers for two high frequencies (confined modes) in three (001) Mo–W superlattices: (4, 4) superlattice, $\nu = 7.06$ THz; (b) (4, 4) superlattice, $\nu = 6.462$ Thz; (16, 4) superlattice, $\nu = 7.06$ THz; (d) (16, 4) superlattice, $\nu = 6.462$ THz; (4, 16) superlattice, $\nu = 7.112$ THz; and (f) (4, 16) superlattice, $\nu = 6.687$ THz.

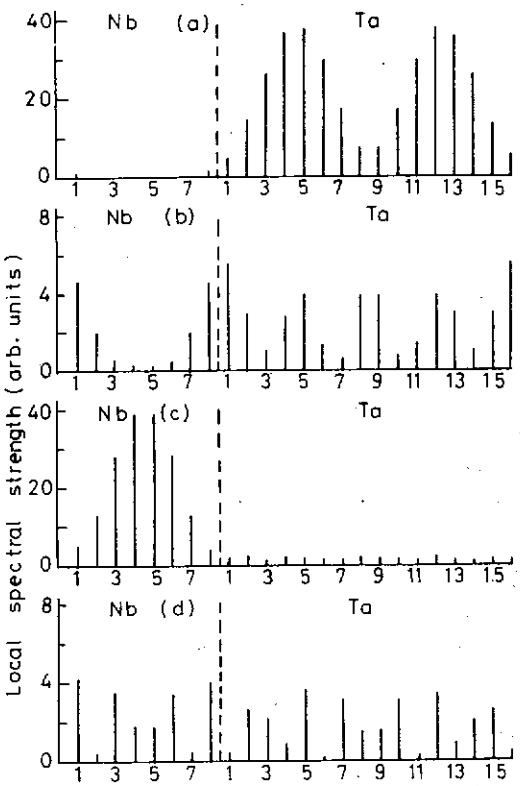

Fig. 17. Spatial variation of the spectral strength (LDOS) for four eigenstates at the Γ-point of a (4, 8) (001) Nb–Ta superlattice, in the neighbourhood of the Fermi level. Energy eigenvalues in (a) −1.52, (b) −1.38, (c) −1.32, (d) −1.16.

easily obtained from the local spectral strength but not from the zeros of the secular determinant (8.25). It is usually better to look for peaks in the local spectral strength, which give the states associated with the zeros of the secular determinant.

As an illustration of this we present in fig. 16 the LDOS of high-frequency phonons for different Mo–W (001) superlattices [50]. This displays the spatial confinement of the high-frequency modes in the Mo layers. In fig. 17 we present the local spectral strength of different electronic states, in the neighbourhood of the Fermi level, for a (4, 8) Nb–Ta (001) superlattice [52]. A rich variety of spatial localization is evident there.

9. Evaluation of Green functions and SGFM formulae for discrete media

In sections 7 and 8 we have seen that in order to proceed with practical calculations by using the SGFM formulae we must be able to calculate Green function elements. These could obviously be obtained by direct calculation of the spectral representation for the bulk Green function [82]. However, even for very simple models direct evaluation of the Green function is not easy [82] and its generalisation for numerical calculations must contend with quickly varying exponential factors. In order to avoid this we have introduced in eqs. (7.22) and (7.23) the transfer matrices for the discrete case, because they provide a fast reliable way to calculate the Green function elements.

9.1. The transfer matrices T, $\bar{T}$, S and $\bar{S}$

The different transfer matrices are defined as follows:

$$G_{n+1,n} = TG_{n,n}\,, \qquad G_{n-1,n} = \bar{T}G_{nn}\,,$$
$$G_{n,n+1} = G_{n,n}S\,, \qquad G_{n,n-1} = G_{n,n}\bar{S}\,. \tag{9.1}$$

In this way we can raise or lower the right or left index at will. It is then clear that we can calculate any Green function element if we know the bulk diagonal element $G_{n,n}$ of the Green function and the transfer matrices, T, $\bar{T}$, S and $\bar{S}$. Transfer matrix techniques have been used in the past to obtain the electronic [83, 84] and vibrational properties [85, 86] of different systems. In earlier versions the calculation of the transfer matrix could require in some cases more than 100 iterations.

Quite recently decimation techniques [87] and fast convergent methods for the transfer matrix calculation [88, 89] have been put forward. The advantage of these methods as compared with the earlier versions is that they only require n iterations where 2^n were needed previously to achieve convergence to the same degree of accuracy. Thus a very substantial saving in computer time is achieved with the new schemes.

Starting from the generic equation

$$-H^{\dagger}_{n,n+1}G_{n-1,n} + (\Omega - H)_{n,n}G_{n,n} - H_{n,n+1}G_{n+1,n} = I\,, \tag{9.2}$$

it is easy to obtain the following relationships between the different transfer matrices:

$$G^{-1}_{n,n} = (\Omega - H)_{n,n} - H_{n,n+1}T - H^{\dagger}_{n,n+1}\bar{T}\,, \tag{9.3}$$

$$H^{\dagger}_{n,n+1}\bar{T} = \bar{S}H_{n,n+1}\,, \tag{9.4}$$

$$H_{n,n+1}T = SH^{\dagger}_{n,n+1}\,. \tag{9.5}$$

It must be noticed that our notation for the transfer matrices differs from that used in [88, 89].

All the different transfer matrices are calculated by using the same iterative procedure, in which some changes in the order in which H_{01} and $H^{\dagger}_{01}$ enter the calculation must be considered [88, 89], and as a byproduct the bulk diagonal Green function elements $G_{n,n}$ are also obtained [88, 90]. From here it is possible to obtain all the different elements $G_{n,m}$ of the Green function needed in the SGFM formulae in order to perform the calculations.

By using the new algorithms usually no more than five iterations are required, and even for very high accuracy in the convergence no more than 15 iterations are needed.

9.2. Evaluating G_s from the constituent transfer matrices

In sections 7 and 8 we have found that $G_s(n, n)$, which is needed to calculate the LDOS, is finally expressed as a function of the bulk diagonal element $G(n, n)$, different powers of the transfer matrices T, $\bar{T}$, S and $\bar{S}$, and of the projection of the system Green function on the interface domain ($\mathcal{G}_s$ or $\tilde{G}_s$), which is also a function of $G(n, n)$ and powers of T, $\bar{T}$, S and $\bar{S}$. So once we know $G(n, n)$ and the different transfer matrices we are able to obtain $G_s(n, n)$.

In the case of the superlattices an increase in the length of the period is reflected in the need to calculate higher powers of the transfer matrices appearing in the SGFM formulation without an increase in the size of the matrices required for the calculation unlike what happens with the diagonalisation of larger secular matrices if one uses the direct diagonalisation procedure associated with supercell schemes.

10. Discrete media: practical aspects

As we have seen the basic SGFM formulae for the single and multiple interfaces are expressed in terms of transfer matrices, which can easily be obtained by means of fast and reliable iterative algorithms [88, 89]. It is now interesting to comment on some practical aspects of this type of calculation, some of which have been used as illustrations in earlier sections.

In order to calculate the transfer matrices and Green function elements a small positive imaginary part was added to the eigenvalue. Different values of the imaginary part can be used and they affect the computer time and some features in the results. In the case of the interface electronic structure we used imaginary parts down to 10^{-5} eV. The use of very small imaginary parts in this case increases considerably the computer time without adding any further essential features. We found that a very good description of the electronic structure and layer LDOS [44, 45] could be obtained with reasonable amounts of computer time by using 0.05 eV as the imaginary part. The iterative scheme to calculate the transfer matrix converged in that case after three or four iterations. As was explained in section 7 the electronic structure and layer LDOS for the two semi-infinite crystals could also be obtained as a byproduct of the interface calculation. The integrals in the two-dimensional Brillouin zone were performed by summing over ten special points [90]. A summation over 64 special points added no important additional features and increased considerably the computer time. Similar conclusions can be reached for the interface phonon case [81].

This is also true in this case of the superlattices, but here we must take into account that how small the imaginary part must be depends on a balance between the accuracy required in the calculation and the computer time employed. When the period of the superlattice increases there will be several modes in a very small energy (frequency) interval and if one uses imaginary parts of the order of, for example, 0.1 eV there will be some difficulty in finding individual peaks when looking at the local spectral strength. In our calculations we employed usually 0.001 eV as the imaginary part and an energy mesh of 0.01 eV or 0.001 eV according to the different situations. This is also true in the case of phonons [50].

References

[1] F. García-Moliner and J. Rubio, J. Phys. C 2 (1969) 1789.
[2] F. García-Moliner and J. Rubio, Proc. Roy. Soc. A 234 (1971) 257.
[3] J.E. Inglesfield, J. Phys. C 4 (1971) L14.
[4] B. Velický and I. Bartoš, J. Phys. C 4 (1971) L104.
[5] F. Flores, F. García-Moliner and J. Rubio, Solid State Commun. 8 (1970) 1069.
[6] V.R. Velasco and F. García-Moliner, Phys. Scr. 20 (1979) 111.
[7] R.J. Jerrard, H. Ueba and S.G. Davison, Phys. Status Solidi b 103 (1981) 353.
[8] I. Bartoš and S.G. Davison, Solid State Commun. 56 (1985) 69.
[9] F. García-Moliner and F. Flores, Introduction to the Theory of Solid Surfaces (Cambridge Univ. Press, Cambridge, 1980).
[10] J.E. Inglesfield, J. Phys. C 10 (1977) 3141.
[11] E. Louis and J.A. Vergés, J. Phys. F 10 (1980) 207.

[12] T.E. Feuchtwang, Phys. Rev. B 13 (1976) 517.
[13] J.E. Inglesfield, J. Phys. C 10 (1977) 4067.
[14] F. García-Moliner, Ann. Physique 2 (1977) 179.
[15] L. Dobrzynski, V.R. Velasco and F. García-Moliner, Phys. Rev. B 35 (1987) 5872.
[16] F. Flores, F. García-Moliner and J. Rubio, Solid State Commun. 8 (1970) 1065.
[17] J.E. Inglesfield and E. Wikborg, J. Phys. C 7 (1973) L158.
[18] J.P. Muscat and G. Allan, J. Phys. F 7 (1977) 999.
[19] I. Bartoš, M. Kollar and G. Paasch, Phys. Status Solidi b 115 (1983) 437.
[20] J.E. Inglesfield and E. Wikborg, J. Phys. F 5 (1975) 1706.
[21] F. Flores, Nuovo Cim. 14 B (1973) 1.
[22] P. Rimbey, J. Chem. Phys. 67 (1977) 698.
[23] V.R. Velasco and F. García-Moliner, Surf. Sci. 67 (1977) 555.
[24] V.R. Velasco and F. García-Moliner, J. Phys. C 13 (1980) 2237.
[25] F. García-Moliner and V.R. Velasco, Phil. Mag. 45 (1982) 299.
[26] G. Platero, V.R. Velasco and F. García-Moliner, Phys. Scr. 23 (1981) 1108.
[27] V.R. Velasco and G. Navascués, Phys. Scr. 34 (1986) 435.
[28] V.R. Velasco and F. García-Moliner, J. Physique Lett. 46 (1985) L733.
[29] V.R. Velasco, Surf. Sci. 128 (1983) 117.
[30] V.R. Velasco and F. García-Moliner, Surf. Sci. 143 (1984) 93.
[31] V.R. Velasco, J. Phys. C 18 (1985) 4923.
[32] V.R. Velasco and F. García-Moliner, Surf. Sci. 161 (1985) 342.
[33] F. García-Moliner and V.R. Velasco, Surf. Sci. 175 (1986) 9..
[34] R.A. Brito, V.R. Velasco and F. García-Moliner, Surf. Sci. 187 (1987) 223.
[35] L. Fernández, V.R. Velasco and F. García-Moliner, Europhys. Lett. 3 (1987) 723.
[36] D.P. Barrio, M.L. Glasser, V.R. Velasco and F. García-Moliner, J. Phys. Cond. Matter 1 (1989) 4339.
[37] H. Rodriguez-Coppola, V.R. Velasco, F. García-Moliner and R. Pérez-Alvarez, 1990, Phys. Scr. 42 (1990) 115.
[38] F. García-Moliner, G. Platero and V.R. Velasco, Surf. Sci. 136 (1984) 601.
[39] G. Platero, V.R. Velasco and F. García-Moliner, Surf. Sci. 152/153 (1985) 819.
[40] G. Platero, V.R. Velasco, F. García-Moliner, G. Benedek and L. Miglio, Surf. Sci. 143 (1984) 243.
[41] A. Levi, G. Benedek, L. Miglio, G. Platero, V.R. Velasco and F. García-Moliner, Surf. Sci. 143 (1984) 603.
[42] F. García-Moliner and V.R. Velasco, Phys. Scr. 34 (1986) 257.
[43] F. García-Moliner and V.R. Velasco, Prog. Surf. Sci. 21 (1986) 93.
[44] M.C. Muñoz, V.R. Velasco and F. García-Moliner, Phys. Scr. 35 (1987) 504.
[45] M.C. Muñoz, V.R. Velasco and F. García-Moliner, Prog. Surf. Sci. 26 (1987) 117.
[46] R. Baquero, V.R. Velasco and F. García-Moliner, Phys. Scr. 38 (1988) 742.
[47] R. Baquero, ICTP Report, Trieste.
[48] F. García-Moliner and V.R. Velasco, Phys. Scr. 34 (1986) 252.
[49] V.R. Velasco, F. García-Moliner, L. Miglio and L. Colombo, Phys. Rev. B 38 (1988) 3172.
[50] R.A. Brito, V.R. Velasco and F. García-Moliner, Phys. Rev. B 38 (1988) 9631.
[51] M.C. Muñoz, V.R. Velasco and F. García-Moliner, Phys. Rev. B 39 (1989) 1786.
[52] V.R. Velasco, R. Baquero, R.A. Brito and F. García-Moliner, J. Phys. Cond. Matter 1 (1989) 6413.
[53] J.R. Sandercock, J. Physique C 5 (1984) 27 and references therein.
[54] R.G. Pratt and T.C. Lim, Appl. Phys. Lett. 15 (1969) 403.
[55] M. Altarelli, in: Heterojunctions and Semiconductor Superlattices, eds. G. Allan, G. Bastard, N. Boccara, M. Lannoo and M. Voos (Springer, Heidelberg, 1986) p. 12;
M. Kriechbaum, in: Springer Series in Solid State Sciences, vol. 67, eds. G. Bauer, F. Kuchar and H. Heinrich (Springer, Heidelberg, 1986) p. 120;
G. Bastard and J.A. Brum, IEEE J. Quantum Electron. QE-22 (1986) 1625.
[56] W. Pötz and D.K. Ferry, Superlatt. Microstr. 3 (1987) 57;
A. Persson and R.M. Cohen, Phys. Rev. B 38 (1988) 5568;
I. Galbraith and G. Duggan, Phys. Rev. B 38 (1988) 10057;
G.T. Einevoll and P.C. Hemmer, J. Phys. C 21 (1988) L1193;
W. Trzeciakowski, Phys. Rev. B 38 (1988) 12493.
[57] O.K. Andersen, O. Jepsen and D. Glötzel, in: Highlights of Condensed Matter Theory, eds. F. Bassani, F. Fumi and M.P. Tosi (North-Holland, Amsterdam, 1985) p. 59;
W.R.L. Lambrecht and B. Segall, Phys. Rev. Lett. 61 (1988) 1764;
J.E. Inglesfield, Prog. Surf. Sci. 25 (1987) 57.
[58] R. Pérez-Alvarez, H. Rodriguez-Coppola, V.R. Velasco and F. García-Moliner, J. Phys. C 21 (1988) 2197.

[59] V.R. Velasco and F. García-Moliner, Phys. Scr. 26 (1982) 405.
[60] V.R. Velasco and F. García-Moliner, Solid State Commun. 33 (1980) 1.
[61] B. Djafari-Rouhani, L. Dobrzynski, V.R. Velasco and F. García-Moliner, Surf. Sci. 110 (1981) 129.
[62] J.E. Inglesfield, J. Phys. F 2 (1972) 878.
[63] E. Louis and F. Yndurain, Phys. Status Solidi b 57 (1973) 175;
M. Elices, F. Flores, E. Louis and J. Rubio, J. Phys. C 7 (1974) 3020;
F. Yndurain and M. Elices, Surf. Sci. 29 (1972) 540;
M. Elices and F. Yndurain, J. Phys. C 5 (1972) L146.
[64] E. Molinari, G.B. Bachelet and M. Altarelli, J. Physique Coll. C4, Suppl. No. 4, 46 (1985) C4-321.
[65] W. Pötz and D.K. Ferry, Phys. Rev. B 32 (1985) 3863.
[66] M. Mora, R. Pérez-Alvarez and Ch. Sommers, J. Physique 46 (1985) 1021.
[67] V.R. Velasco, F. García-Moliner, H. Rodriguez-Coppola and R. Pérez-Alvarez, Phys. Scr. 41 (1990) 375.
[68] F. García-Moliner, R. Pérez-Alvarez, H. Rodriguez-Coppola and V.R. Velasco, J. Phys. A 23 (1990) 1405.
[69] P.G. de Gennes and D. Saint-James, Phys. Lett. 4 (1963) 151.
[70] S. Yoksan and A.D.S. Nagi, J. Low Temp. Phys. 66 (1987) 115.
[71] R.L. Kobes and J. Whitehead, Phys. Rev. B 36 (1987) 121.
[72] F. Stern, Phys. Rev. B 5 (1972) 4891; Crit. Rev. Solid Sci. 4 (1974) 499.
[73] L.R. Ram-Mohan, K.H. Yoo and R.L. Aggarwal, Phys. Rev. B 38 (1988) 6151.
[74] B.T. Smith et al., Matrix Eigensystem Routines – EISPACK Guide, 2nd Ed., Lecture Notes in Computer Science, vol. 6 (Springer, New York, 1976).
[75] J.T. Dongarra et al., LINPACK Users Guide (Society for Industrial and Applied Mathematics, Philadelphia, 1979).
[76] C. Moler and C. van Loan, SIAM Rev. 20 (1978) 801.
[77] W.H. Press, B.P. Flannery, S.A. Teukolsky and W.T. Vatterling, Numerical Recipes. The Art of Scientific Computing (Cambridge Univ. Press, New York, 1987).
[78] L.V. Atkinson, P.J. Harley and J.D. Hudson, Numerical Methods with FORTRAN 77: A Practical Introduction, International Computer Science Series (Addison-Wesley, Reading, MA, 1989).
[79] J. Pollman and S.T. Pantelides, Phys. Rev. B 21 (1980) 709.
[80] D.J. Chadi, Phys. Rev. B 16 (1977) 790.
[81] R.A. Brito-Orta, V.R. Velasco and F. García-Moliner, Surf. Sci. 209 (1989) 492.
[82] S. Katsura, T. Norita, S. Inawashiro, T. Horiguini and Y. Abe, J. Math. Phys. 12 (1971) 892.
[83] L.M. Falicov and F. Yndurain, J. Phys. C 8 (1975) 147.
[84] F. Yndurain and L.M. Falicov, Phys. Rev. Lett. 37 (1976) 928.
[85] F. Yndurain and P.N. Sen, Phys. Rev. B 14 (1976) 531.
[86] V.R. Velasco and F. Yndurain, Surf. Sci. 85 (1979) 107.
[87] F. Guinea, C. Tejedor, F. Flores and E. Louis, Phys. Rev. B 28 (1983) 4397.
[88] M.P. López Sancho, J.M. López Sancho and J. Rubbio, J. Phys. F 14 (1984) 1205.
[89] M.P. López Sancho, J.M. López Sancho and J. Rubio, J. Phys. F 15 (1985) 851.
[90] S.L. Cunningham, Phys. Rev. B 10 (1974) 4988.